Future Directions of High-Fidelity CFD for Aero-Thermal Turbomachinery Research, Analysis and Design

Gregory M Laskowski[1] & Jim Kopriva[2]
GE Aviation, Lynn MA 01905

Vittorio Michelassi[3] & Sriram Shankaran[4]
GE Aviation, Evendale OH 45215

Umesh Paliath[5] & Rathakrishnan Bhaskaran[6]
GE Global Research, Niskayuna NY 12309

Qiqi Wang[7] & Chaitanya Talnikar
Massachusetts Institute of Technology, Cambridge MA 02139

ZJ Wang[8] & Feilin Jia
University of Kansas, Lawrence KS 66045

Computational Fluid Dynamics is a powerful tool used on a daily basis by designers and researchers in the advancement of propulsion technology. As hardware and software technology continue to evolve, the impact on propulsion systems has the potential to be disruptive. With continued development of High Performance Computing, Large Eddy Simulation, High-Order unstructured grid algorithms, optimization and uncertainty quantification it is conceivable that a new frontier of simulation based research, analysis and design capability is in the foreseeable future. In order to accelerate this development collaboration between industry, academia and government labs is required.

Nomenclature

BR	=	Bypass Ratio
c	=	Chord Length
CFD	=	Computational Fluid Dynamics
DNS	=	Direct Numerical Simulation
HLES	=	Hybrid Large Eddy Simulation
HO	=	High-Order
HPC	=	High Performance Computing
HPC	=	High Pressure Compressor
HPT	=	High Pressure Turbine
IDDES	=	Improved Delayed Detached Eddy Simulation
IDDES-T	=	Improved Delayed Detached Eddy Simulation with Transition
LES	=	Large Eddy Simulation
LPC	=	Low Pressure Compressor
LPT	=	Low Pressure Turbine
Ma	=	Mach Number

[1] Principal Engineer high-fidelity CFD, Advanced Design Tools, 1000 Western Ave MS74301, AIAA Member.
[2] Senior Engineer, 1000 Western Ave MS74301.
[3] Chief Consulting Engineer.
[4] Aero-thermal Subsection Manager.
[5] Project Leader for high-fidelity CFD.
[6] Lead Engineer.
[7] Associate Professor, Department of Aeronautics and Astronautics.
[8] Spahr Professor & Chair of Aerospace Engineering. AIAA Fellow.

MDAO = Multi-Disciplinary Analysis and Optimization
OPR = Overall Pressure Ratio
Pt = Total Pressure
RANS = Reynolds Averaged Navier Stokes Equations
Re = Reynolds number
Ro = Rossby Number
S = Slot Height
S1B = Stage 1 Blade
S2B = Stage 2 Blade
S1N = Stage 1 Nozzle
S2N = Stage 2 Nozzle
SFC = Specific Fuel Consumption
St = Strouhal Number
TIT = Turbine Inlet Temperature
Tt = Total Temperature
TVD = Total Variation Diminishing
UQ = Uncertainty Quantification
URANS = Unsteady Reynolds Averaged Navier Stokes Equations
VKI = von Karman Institute
WMLES = Wall-Modeled Large Eddy Simulation
WRLES = Wall-Resolved Large Eddy Simulation

I. Introduction

Gas turbines are, and will continue to be, the backbone of narrow and wide body aircraft propulsion. The main reason for the success of gas turbines is their power density, i.e. thrust per unit engine weight, and their efficiency. The US alone consumed approximately 35.6 billion gallons of aviation fuel in 2012 (FAA, 2014). Technologies that can further improve fuel efficiency while reducing emissions and noise can have a significant impact on the US economy. As aircraft engines continue to evolve, supercomputing, optimization and CFD will play an increasingly important role in further improving both thermal and propulsive efficiencies in a cost effective manner.

The modern high bypass turbofan engine is based on the Brayton cycle. Air is ingested in the engine and passes through the fan. A majority of the flow bypasses the core of the engine to increase the propulsive efficiency (refer to Figure 1). The core flow is compressed in the compressor increasing P_t and T_t. Fuel is added and burned in the combustor increasing T_t and slightly reducing P_t and the flow is expanded through the turbine reducing P_t and T_t. Work extracted by the turbine drives the compressor. The turbine also drives a fan at the front of the engine in order to increase the mass flow through the engine thus increasing the propulsive efficiency. In order to improve thermal efficiencies the turbine inlet temperature and compressor pressure ratio have historically increased nearly linearly with time.

A modern high bypass turbofan engine is depicted in Figure 1. Each module shown in Figure 1 has unique engineering challenges and they all contribute to engine efficiency, operability, reliability, emissions and cost. The fan is a single blade row consisting of many blades, has a high Reynolds number based on chord and experiences a wide range of Mach numbers. Tip clearances can be very small and secondary flows in the hub and tip are critical for performance. The compressor sits downstream of the fan and consists of multiple alternating rows of stationary and rotating airfoils and experiences an adverse pressure gradient over the stages. The Reynolds and Mach numbers are in the turbulent and compressible regimes and the total airfoil count can easily exceed 1000.

Like the compressor, the turbine consists of alternating rows of stationary and rotating airfoils on the order of 100-1000. The Reynolds and Mach numbers can vary from laminar to turbulent and weakly compressible to fully compressible respectively depending on the machine and stage. Unlike the compressor, turbine stages experience a favorable pressure gradient for most of the airfoil, and the front end of the turbine, sitting downstream of the combustor, experiences very high temperatures that requires extensive cooling to ensure durability. In order to achieve this, flow is extracted from the compressor, bypasses the combustor and is used for internal convection, impingement and film cooling. Minimizing the amount of cooling flow is a systems level consideration, while reducing film mixing losses and ensuring durability is an aero-thermal component level consideration.

The secondary flow cooling supply system consists of pipes and geometrically complex seals, cavities and turning vanes and encompasses a wide range of Rossby, Reynolds and Mach numbers. For the turbomachinery modules the large rotational rates (1000's to 10,000's of RPM's, with tip speeds above 300 m/s), together with small

seal clearances provide additional engineering challenges and can result in costly maintenance and reduced SFC if not properly designed and understood (Lattime and Steinetz, 2002).

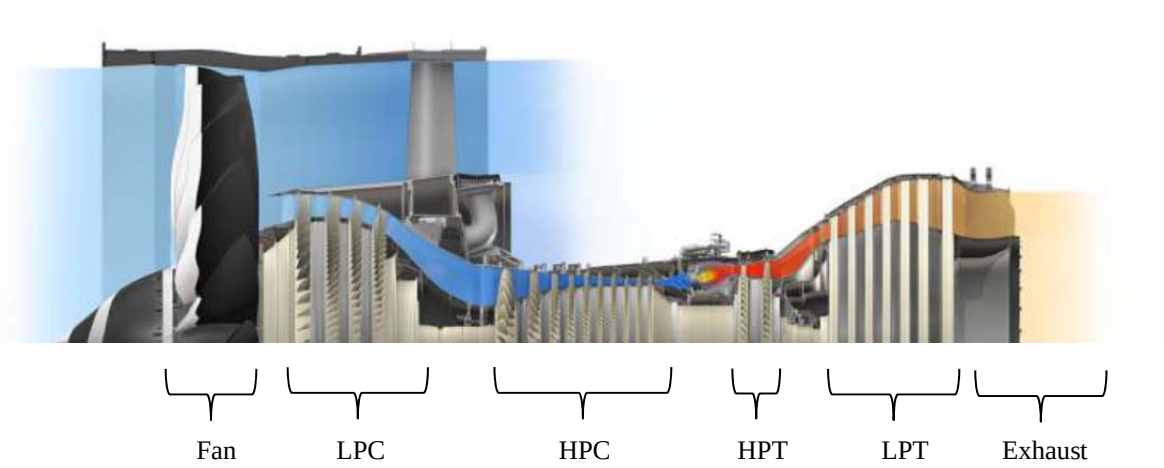

Figure 1. Modern turbofan engine.

The proper handling of boundary conditions in turbomachinery for aero-thermal problems is an important consideration for design. This can be a challenge due not only to the large airfoil counts, number of stages and ranges of non-dimensional numbers noted previously but also due to non-integral counts important for the azimuthal direction and frame change between stator and rotor, important for the axial direction as illustrated in Figure 2. Leakage flows, flow extraction in the compressor and flow addition in the turbine further complicate the landscape. Furthermore, boundary conditions can vary widely over a transient mission.

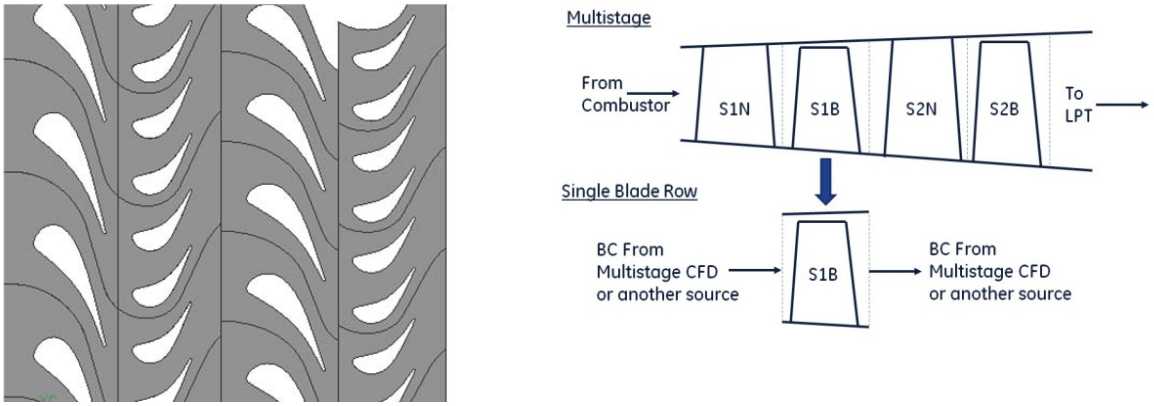

Figure 2. Boundary condition challenges for a generic 2-stage HPT. (Left) Pitchwise periodicity due to airfoil counts. Stage 1: integral count. Stage 2: non-integral count. (Right) Streamwise interface due to rotation. Multi-stage vs single blade row.

The geometry being considered for analysis in design is another critical consideration. Transient missions noted earlier not only impact boundary conditions, but can also result in deformations of the hardware. Thermal and mechanical stresses can have a first order impact on clearances and leakage flows. Service degradation after many cycles is yet another aspect of how geometry may change over time: fan surfaces may deform due foreign object ingestion (Schnell et al., 2014), compressor tip coatings may erode (Elmstrom et al., 2011), and high pressure turbine surface roughness can vary widely (Bons et al., 2001). Another important consideration in terms of geometry is manufacturing variation that can result in significant part-to-part and engine-to-engine variation. For example, Bunker (2009) executed a Monte Carlo simulation for a simplified model and showed film cooling hole diameter variation of 10% can reduce blade life by 33%. Furthermore, non-uniform coatings of compressor and

turbine airfoils presents another challenge. Slight perturbations can impact the aero-thermal performance of the components (Montomoli, 2015). At some level uncertainty quantification is necessary to ensure a robust design. Figure 3 illustrates the concept for robust design. As an example, three different geometries are being explored to achieve an outcome. Geometry 1 achieves the highest possible performance but is on a cliff and any variation in the geometry will result in rapidly deteriorating performance. Geometry 3 achieves 95% the performance of Geometry 1 and remains robust over a much larger variation of the critical parameters. This simple example illustrates the need to account for variation in real design and not doing so can adversely impact SFC, emissions or durability. Uncertainty Quantification (UQ) is an active area of research and good examples can be found in Montomoli (2015).

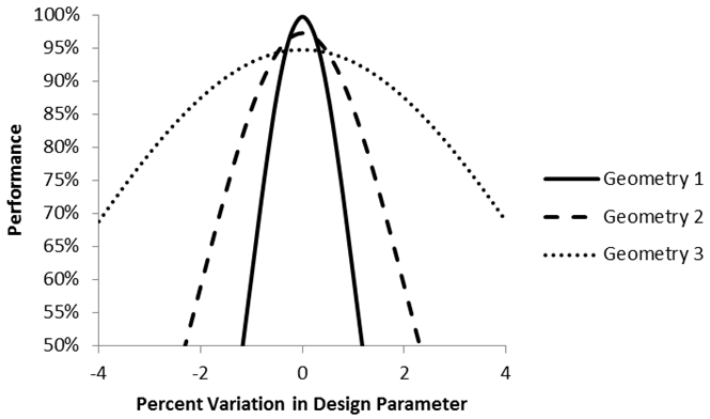

Figure 3. Example of robust design showing three different geometries designed to achieve a design objective.

Boundary conditions and geometry modeling is critical to aero-thermal design of gas turbines. The wide range of Re, Ro and Ma for the various features, components and systems of an engine result in complex unsteadiness, both deterministic and stochastic, buoyancy and shocks respectively. Design tools need to account for complex physics, the interaction of these phenomena while addressing the boundary condition and geometry challenges noted earlier, and they need to be fast.

I.1 Motivation: The Problem

Design tools need to balance speed and accuracy and CFD currently cannot compete with the speed of empirically based 0D and 1D flow network solvers. Correlations and empirical tools will likely continue to be a part of the design process for years to come. It is important to point out that in order to overcome accuracy issues with 0D and 1D tools, large and expensive rig tests are required to evolve and certify the design of an engine.

Over the past several decades a CFD ecosystem has evolved consisting of geometry cleanup, mesh generation, physics models for turbulence, boundary conditions for turbomachinery, algorithms for solution of PDE's, optimization, post-processing, HPC and most recently UQ. This ecosystem has matured to the point where it has become indispensable in the design of aircraft engines and has become commonplace in the design guidance of new technologies and products. But the perception of CFD continues to suffer from a "love/hate relationship" due to the cost saving opportunities and potential for misses due to a lack of a complete validation respectively (Warwick, 2014). In order for CFD to be adopted, effective and trusted validation is required over a broad design space. This can be challenging for aircraft engines due to the large number of airfoils, frame changes, range of Re and Ma, high temperatures and pressures as well as uncertainty due to manufacturing variation and transient missions noted earlier.

Fischberg et al. (1995) noted a RANS based design system contributed to 0.6% gain in fan efficiency and 1% gain in LPC efficiency while saving $20M in rig testing. Fischberg et al. (1995) also noted a RANS based redesign of an HPC system contributed to 2% improved efficiency, cost savings of $17M in reduced rig testing and redesign time cut in half. Another often quoted example of the impact CFD has had in the aerospace industry is Boeing's reported reduction of wind tunnel wing tests from 70-80 in the 1980's to 11 in the mid 1990's followed by a long plateau (US Department of Energy, 2010). CFD has also "helped reduce the number of expensive high-pressure rig tests required for certification of jet engines by 50% at Pratt & Whitney in a similar timeframe wherein Boeing's use of CFD led to fewer wind tunnel tests. However, as in the case of Boeing, Pratt & Whitney has seen only a 10% further reduction in the required engine tests in the past decade" (US Department of Energy, 2010). One perception based on these reports is that the RANS and URANS model development has plateaued for these examples because

of shortcoming in the turbulence physics modeling approaches (Moin, 2014). In order to extract maximum value from the RANS/URANS process, GE Aviation is focusing on improvements to the CFD ecosystem and the ability to quickly and repeatedly model more complex geometries. Furthermore, HPC enabled variants of LES will likely be the next major contributor to design and reduced testing (Moin, 2014). Moin goes on to note that, while computationally intensive, WMLES is already used in the combustion community. While it is true that variants of LES have been adopted at some level by the combustion community, the turbomachinery and heat transfer communities have been slower to adopt these methods due to the high computational cost associated with high Re wall bounded flows. Recently very targeted applications have been reported in this area. (Gourdoin et al., 2014; Rodebaugh et al., 2015; Ivanova and Laskowski, 2015; Zlatinov and Laskowski, 2015; Michelassi et al., 2014).

Opportunities for reduction in rig testing are not the only motivating factor for advancing high performance computing, algorithms and physics models. With the advent of new manufacturing processes and advanced materials, the traditional design space for aircraft engines will open up requiring advanced design methods to exploit the opportunities these advances provide. One example is additive manufacturing which is already being utilized for certain components and has the potential to enable advanced cooling and heat exchanger technologies among other things. Another clear example is ceramic matrix composite (CMC) which will enable hotter temperatures in the hot section. As manufacturing and materials capabilities continue to mature it is very likely that HPC enabled highly automated high-fidelity CFD along with multi-disciplinary optimization methods have the opportunity to contribute to advanced designs, reduced SFC, increased durability, reduced NOx and reduced noise.

I.2 Algorithms and Physics Modeling

Geometry modeling and grid generation are bottlenecks that can adversely impact speed of an analysis. In order to maximize the impact CFD can have in design, the entire ecosystem (pre-processing, solver and post-processing) needs to be considered. As noted previously the need for speed will mandate the use of RANS and URANS based CFD for years to come. In order to enable automation for optimization high quality unstructured grids will undoubtedly be utilized. From an accuracy perspective, it is foreseeable that some variant of wall-resolved, wall-modeled or hybrid RANS/LES will see growing use for critical problems that require the fidelity and cost savings opportunities when compared to rig tests. As HPC, algorithms and physics models, most notably wall models, continue to improve it is likely variants of LES will continue to penetrate deeper into the design of components and systems.

In order to enable speed, unstructured grid capability will most likely be a requirement. In order to ensure accuracy of LES, algorithms that minimize both dispersive and dissipative error will be needed. As noted by Lopez-Morales (2014), significant advances in High-Order methods over the last 20 years has resulted in robust, efficient and accurate high-order schemes that will support development of new and emerging aircraft roles. The ideas are also valid for internal flows and are the focus of numerous recent studies relevant to the gas turbine industry (Michelassi et al., 2014; Lu and Dawes, 2015; Mangani et al., 2015; Wiart et al., 2015; Rodebaugh et al., 2015; Garal et al., 2015; Marty et al., 2015; Pichler et al., 2016). Various solution algorithm techniques have emerged in support of higher fidelity turbulence modeling (e.g. LES) including 2^{nd} order bounded central difference commonly found in commercial solvers, 2^{nd} order low dispersive/dissipation schemes (Khalighi et al., 2010), spectral difference (Cassagne et al., 2015), Discontinuous Galerkin (Schwaenen et al., 2010; Duggleby et al., 2013), or flux reconstruction/CPR schemes (Huynh et al., 2013; Lopez-Martinez et al., 2014). Furthermore, as LES moves from being an analysis tool to design tool automation will be required to facilitate optimization and trade studies thus further motivating the need for unstructured capability.

One challenge in simulating turbomachinery flows is the wide range of length and time scales. Flows in compressors and turbines are inherently unsteady. The flow has both stochastic and deterministic unsteady sources, the former being true turbulence, while the latter is generated by stator-rotor interaction, vortex shedding, shock motion, and potential effects. In sections to follow examples of how deterministic and stochastic unsteadiness co-exist (discrete wakes in LPT and vortex shedding generating pressure waves in HPT). Reynolds-averaged based methods filter out the stochastic unsteadiness and replace its effect onto the averaged flow field with the modelled Reynolds stresses. With reference to Figure 4, the residual deterministic unsteadiness is either filtered out, reintroduced in terms of “deterministic stresses”, or resolved by URANS to capture up to blade-passing frequencies. These methods can ensure fair accuracy as long as there is a clear frequency gap between the deterministic frequencies and the frequencies associated with turbulence, i.e. in area of inertial subrange, as the Reynolds averaging process is not designed to capture the interaction of deterministic and stochastic unsteadiness. Figure 4 shows that if the unsteady flow spectrum moves from the black to the red curve, when the deterministic frequency is high, we can expect turbulence modelling difficulties. LES and DNS sit at the rightmost limit, and they indeed ensure high-accuracy provided the resolution in space and time is appropriate, but there is also an intermediate

approach, called hybrid, in which LES is blended with URANS that apply only to boundary layers, the most grid intensive regions in wall driven flows, thereby relaxing grid requirements.

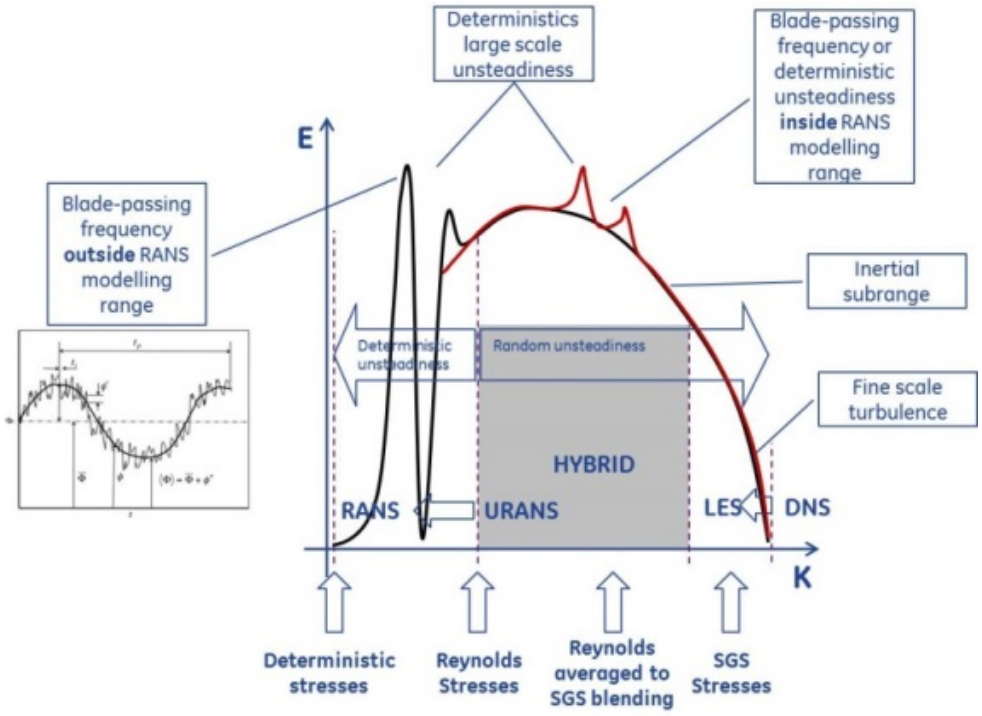

Figure 4. Filtering unsteadiness in turbomachinery.

I.3 High Performance Computing

Broad industry surveys such as Mustain et al. (2014) and Ezell and Atkinson (2016) show that most enterprises view HPC as critical to their R&D efforts and therefore future competitiveness. There is also broad agreement that a 1,000-fold increase in computing capability and capacity could be consumed in a relatively short period of time. Aerospace can certainly be included in these conclusions. Slotnick et al. (2014) provide a detailed vision and series of recommendations to enable transformational CFD capability for the aerospace industry by the year 2030 as HPC continues to advance. Six key technology areas were identified (1) High Performance Computing, (2) Physical Modeling, (3) Numerical Algorithms, (4) Geometry and grid generation, (5) Knowledge Extraction and (6) MDAO. In addition, four Grand Challenge problems were identified, one of which was “off-design turbofan engine transient simulation”. Gourdain et al. (2014) project LES to become a standard design tool for gas turbine applications in the 2030’s but admit their projection is based on past evolution of HPC growth and may be inaccurate. Moin (2014) suggests wall-modeled LES executed on a 5-exaflop / s machine has the potential to enable not just one off analysis but opportunity to design and optimize. In July 2015 President Obama launched the National Strategic Computing Initiative with the objective to (1) accelerate delivery of exascale computing, (2) align technologies for modeling and simulation with big data analytics (3) develop roadmap for “post- Moore’s Law” (4) continue development in the US HPC ecosystem (5) drive collaboration between Government, industrial and academic sectors. A meaningful grand challenge program that would resonate with aircraft engine industry is successful execution of MDAO of a turbomachinery system using high-fidelity CFD including validation which would then be demonstrated on a well instrumented technology demonstrator. By validating the capability of combining HPC and high-fidelity CFD to design complex systems, there is a tremendous potential for cost reduction and further investment by industry. As described by Gara and Nair (2010), a holistic view of the entire HPC ecosystem will be required to fulfill this promise including strong collaboration between developers and users. On the software side, improvements will be needed in every step of the HPC process including from CAD model to mesh, efficient run scheduling and monitoring, adaptive handling of a mix of heterogeneous nodes, as well as insightful post-processing of exabyte scale databases."

I.4 Performance

The role of high-fidelity CFD in reducing gas turbine fuel consumption can be better understood by observing how producing thrust by GT is governed by four different efficiencies:

A. Thermodynamic efficiency. Gas turbines are based on the Brayton cycle, the efficiency and performance of which are directly proportional to pressure ratio and firing temperature.
B. Aerodynamic efficiency. Compressor, high-pressure and low-pressure turbines control the quality of imparting and extracting energy from the working fluid, and guarantee operability range.
C. Thermal efficiency. GT firing temperatures are often above materials capability, requiring internal cooling and external shielding of combustor and high-pressure-turbine parts from hot gases.
D. Propulsive efficiency. The quality of the process of generating thrust is inversely proportional to the fan pressure ratio, and directly proportional to the volume flow.

CFD plays a key role in each of the four points above. In fact, the aerodynamic efficiency of a gas turbine governs the irreversibilities of the energy exchange between fluid and blades, and more generally wetted surfaces. CFD is also routinely used to predict operability ranges, cooling and purge systems, fan and nacelle aerodynamics, all essential requisites for a successful propulsion system.

However the full potential of CFD has not been fully realized due to challenges in capturing the details of gas turbine flows. Flow unsteadiness in turbomachinery is both stochastic, i.e. turbulence driven, and deterministic, i.e. stator-rotor periodic interaction driven. The interaction of the two frequency ranges poses a formidable task both in case one decides to model or to resolve this process. Despite the difficulties, design iterations are generally accomplished by modeling all scales of turbulence with RANS or URANS (Unsteady Reynolds Averaged Navier-Stokes), the latter being used when capturing the large scale unsteady interaction between blade rows is deemed necessary. While fast, these methods suffer from accuracy issues in the presence of complex mixing processes (Michelassi et al., 2015) which limits the true benefit CFD can have on design optimization and technology development. Alternatively, resolving the turbulent unsteady flow field in gas turbine through Direct Numerical Simulation (DNS) or Large Eddy Simulation (LES) has been shown to be very accurate, but upwards of 100x more computationally expensive (Sandberg et al., 2015; Michelassi et al., 2015; Wheeler et al., 2015)) even with simplified geometries. Measurements are another route to get insights into the flow field in GT, but they are expensive and often unable to provide enough details into the underlying physics. As a result, designers incorporate margins into their calculations to ensure adequate performance and component life during operation to compensate for the aero-thermal loading uncertainty partly caused by CFD inaccuracies. As improvements to the ecosystem and HPC continue to evolve the potential impact on time to market, cost of development, durability, SFC and noise can be profound.

II. Example Applications of High-Fidelity Aero-thermal CFD in Aircraft Engines

In order to project a path forward for CFD it is important to understand the current status. Clearly, RANS and URANS will continue to be the workhorse of design for many years to come. Equally clear is the fact that the next generation of CFD will be some variant of LES, namely hybrid RAN/LES or wall-modeled LES, along with optimization and UQ capabilities. A brief discussion of recent activities in these areas will be discussed.

II.1 Exhaust Jet Noise

Jet noise is one of the most dominant noise components from an aircraft engine that radiates over a wide frequency range. Empirical and semi-empirical models that rely on scaling laws and calibrations of constants based on far field acoustic measurements are limited in their range of applicability, especially for complex 3D exhaust systems. In the past decade, using LES for time accurate prediction of turbulent near-field flow and coupling with far-field propagation for jet noise prediction has gained increasing traction in the jet noise community (Bodony et al., 2008). With the continuous advances in numerical algorithms and computer hardware, this direct jet noise prediction approach has become more and more affordable.

GE Aviation has developed a similar LES based approach (Paliath et al., 2011) to accurately predict the acoustic signature from complex exhaust nozzles and noise control devices such as dual stream and chevron nozzles an example of which can be found in Figure 5. GE Aviation has also extended the predictive capability to canonical jet-installed configurations (Paliath et al., 2013) shown in Figure 5. It is essential to be able to predict and understand the altering of the noise source generation and propagation mechanisms in the presence of forward flight and installation geometries like pylon, wing and flap. Such knowledge is vital to engine and airframe integration,

and is extremely difficult and costly to acquire through experiments. An accurate, efficient and robust LES approach coupled with high performance computing provides an attractive alternative.

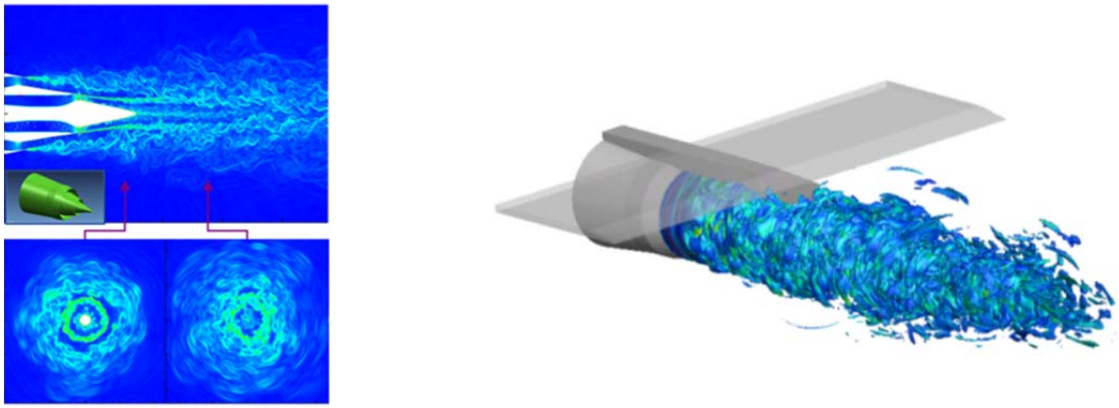

Figure 5. Large Eddy simulations of exhaust nozzles. (Left) Density gradients from dual flow exhaust nozzle simulation. (Right) Q-contours from simulation of dual flow nozzle with pylon and wing surface.

II.2 Compressor

Compressors and turbines share similar challenges in terms of unsteadiness driven by rotor-stator interaction, clearances, boundary layers and wakes. The difference is the nature of the pressure gradient, primarily adverse that is responsible for the fairly narrow operability range as compared with turbines. Nowadays, conventional CFD is being used to predict the onset of stall in axial compressors, generally working with single blade row and proceeding to multistage with some empiricism dictated by the inability to accurately compute boundary layer and endwall flows in adverse pressure gradients. Axial compressor design is often driven by proprietary correlations, and the penetration of CFD in compressor design is once again limited by accuracy, but for aircraft engine compressors also by the inability to predict post-stall behavior, essential information in the design of high-pressure-ratio core compressors. Leggett et al. (2016) attempted to use LES of a simple compressor airfoil to predict off design performance at both positive and negative incidence as shown in Figure 6. They observed how, while single blade row loss levels predicted by RANS are in fairly good agreement with a high-resolution LES, LES and RANS predict very different wakes, as a result of differences in the growth of suction and pressure side boundary layers subject to adverse pressure gradients. Variants of LES are able to predict the growth of large scale unsteadiness in presence of shear layers with or without pressure gradients. This capability would allow CFD to cover the full operability range of a compressor, including post stall.

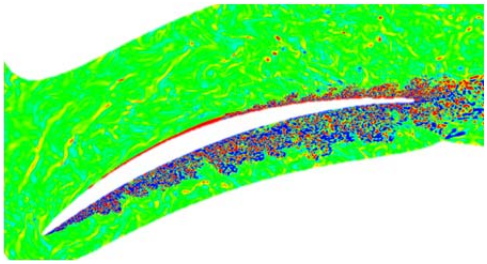

Figure 6. Wall-resolved Large Eddy Simulation of a spanwise and pitchwise periodic compressor blade at negative incidence.

Looking ahead, the computational requirements for realistic compressor multi-stage simulations with LES presents some daunting challenges. As noted by Gourdain (2014) the cost ratio from RANS to wall-resolved LES for Reynolds numbers on the order of 1e6 is about 1e4 and they project LES to become a standard design tool by 2030 if Moore's Law holds. Figure 7 shows the computational estimate for different kinds of simulations of interest to compressor aerodynamics. These estimates were made assuming an optimistic view that compute power

will increase by a factor of 1000x over the next 10 years. While URANS simulations of a full compressor can potentially be achieved on National Lab machines today, the outlook for LES simulations beyond single blade-row are a decade out. This further emphasizes the need for investment, research and advances in the underlying numerical algorithms, physics modeling and computer science infra-structure.

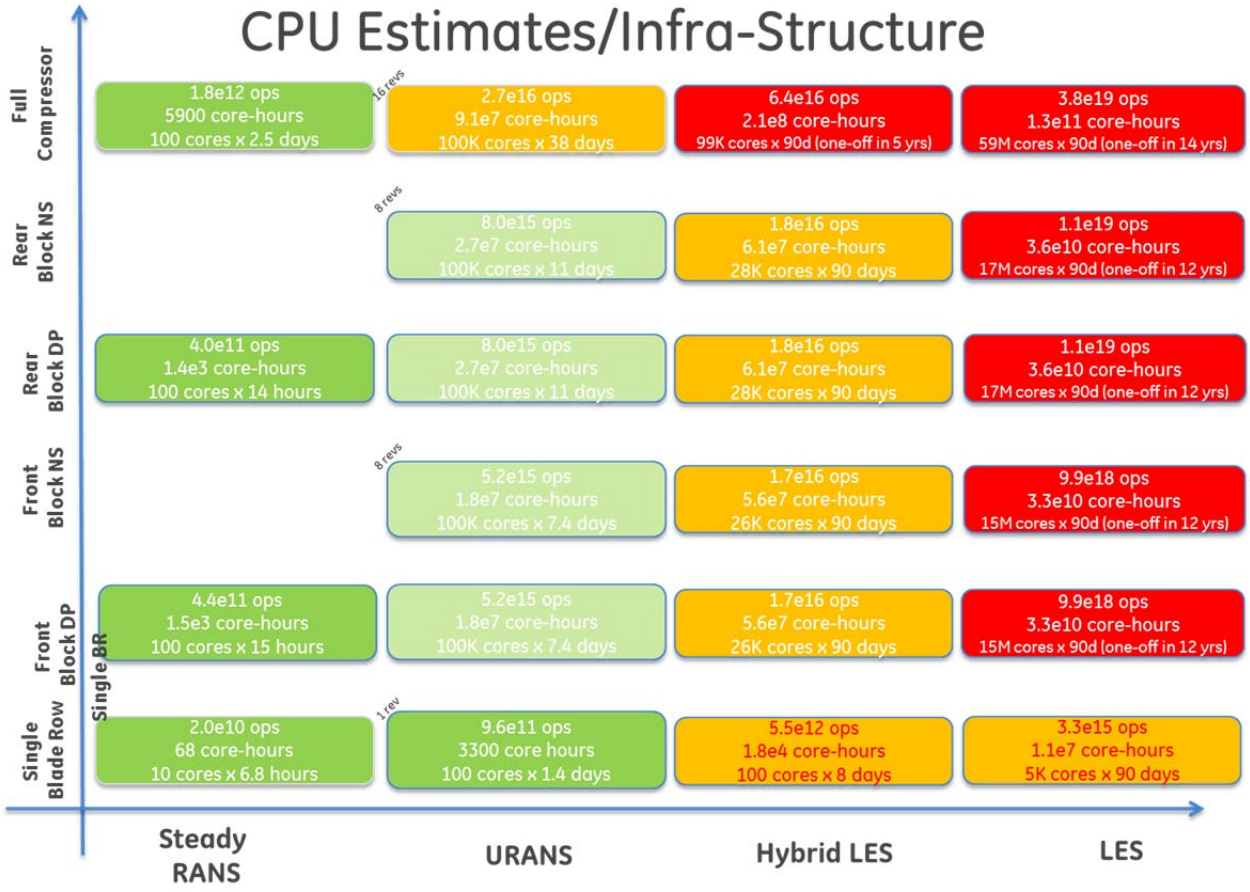

Figure 7. Computational estimates for compressor simulations of various levels of fidelity. Red boxes correspond to simulations that are possible in > 5 years, orange boxes in 1-5 years on modest sized supercomputers, and green boxes are plausible on today's linux clusters.

II.3 Low Pressure Turbine

As an example of how high-fidelity CFD will impact future development, Low-Pressure-Turbines (LPT) aerodynamics has been deeply scrutinized to investigate the impact of turbulence and large scale unsteadiness on performance. LPTs are among the best candidates due to their moderate Reynolds number (from 50K for narrow body up to 300K for wide body), and due to their performance derivative. The intermittent nature of the flow, driven by both wake-profile interaction and potential effects, has been studied by numerous authors (Denton, 1993); Arndt, 1993), and shown experimentally by Halstead at al. (1997). Depending on the various combinations of flow coefficient, reduced frequency, stator-rotor axial gapping, the unsteady interaction can add or mitigate losses. Michelassi et al. (2003) compared DNS, LES, and URANS in a typical wake-profile interaction. The investigation anticipated the difficulties discovered by Medic and Sharma (2012) when attempting to predict LPT profile losses with RANS. These investigations motivated the further application of DNS and LES to LPT flows, like those of Sandberg et al. (2015) and Michelassi et al. (2015).

The LPT unsteady loss generation mechanism was scrutinized by Michelassi et al. (2015). The concerted effect of both reduced frequency and flow coefficient was analyzed first by DNS, then by LES validated with DNS results of the T106A LPT profile by Stadtmueller and Fottner (2001). Losses were analyzed using Denton's control volume approach with DNS and LES results. The impact of incoming wakes at a fixed flow coefficient is summarized in Figure 8. The curve shows the difference between the mixed out losses computed by using Denton method, and the

mixed out total losses, computed by using flow quantities extracted upstream and downstream of the profile using the DNS results. In the absence of wakes, the two methods gives the same value, while the difference peaks at F_{red}=0.3-0.6, regardless of the Reynolds number and turbulence intensity. The difference becomes again negligibly small for large F_{red}. This important result shows how unsteadiness can increase steady losses, but for high F_{red}, the effect is mitigated as wakes merge together before reaching the LPT profile.

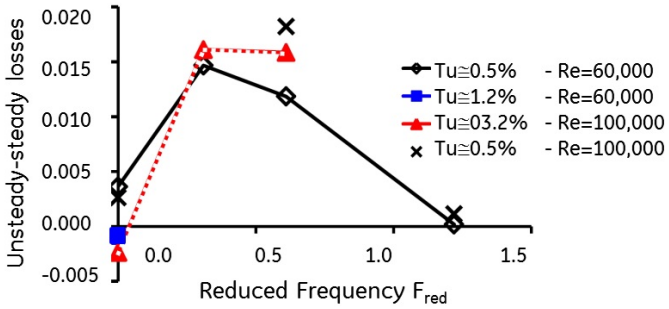

Figure 8. Unsteady losses as a function of reduced frequency for the T106A profile at Re=60K and 100K.

This result was confirmed by extending the investigation to the concerted action of F_{red} and flow coefficient, Φ (Michelassi et al., 2015), two key design parameters engineers need to optimize. The results of the LES revealed how the unsteady losses generation depends on the normal distance between wakes as depicted in Figure 9. This result is important as it shows how the decision on vane and blade count, revolution speed, and spanwise height can have an impact on the unsteady loss generation, and should be carefully weighed in the early design phase. Unfortunately, the inability of RANS and URANS to predict wakes decay poses severe limitations to the use of low-order models.

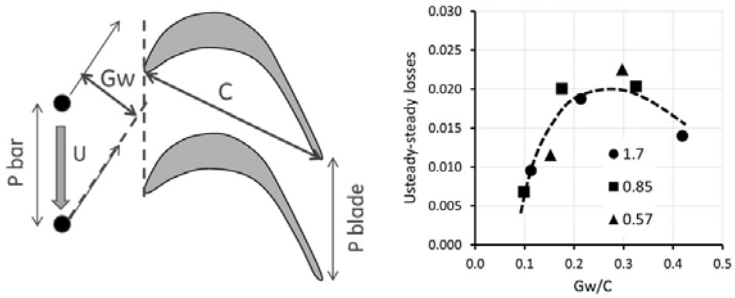

Figure 9. Unsteady losses as a function of both reduced frequency and flow coefficient for the T106A profile at Re=100K.

II.4 High Pressure Turbine

Numerical simulations of the flow in High-Pressure Turbines (HPT) is one of the greatest challenges to modern CFD, since the HPT operates at both transonic Mach numbers high Reynolds numbers and is extensively cooled both internally and with film which can impact the aerodynamics of the stage. The importance of the correct prediction of the aero-thermal load of HPT is crucial to both performance and durability of modern aircraft engines. In order to execute insightful and engineering quality LES of a single blade row fully cooled S1B we estimate approximately 20M core hours on OLCF Titan would be required. The cost increases substantially if simulations of multiple stages with non-integral counts are required. While not currently practical for design, opportunities do exist to focus on important aspects of the system or component level analyses using a building block approach.

As an example, Kopriva et al. (2014, 2015) conducted a detailed study of the uncooled VKI S1N of Arts et al. (1992) focusing on SST, IDDES, IDDES with a transition model and WALE LES in ANSYS Fluent. Simulations were conducted on unstructured meshes consisting of triangular elements. Various levels of agreement with wake data were reported depending on the modeling approach as shown in Figure 10. Clearly transition is an issue, but so too is turbulence mixing in the wake. Figure 11 highlights the impact of inlet turbulence on the downstream wake. A data comparison is first made for the case with ~0% inlet turbulence. As the turbulence is increase to 6%, earlier transition occurs on the suction side of the S1N resulting in a thickened wake. Increasing the inlet turbulence to 20% results in an increased spreading of the wake and mixing losses growing further into the core flow. Kopriva et al.

(2014) executed the same modeling study at ~0% inlet turbulence for the trailing edge cooled VKI S1N of Kapteijn et al. (1996) and found, not surprisingly, a similar trend to the uncooled results as shown in Figure 12.

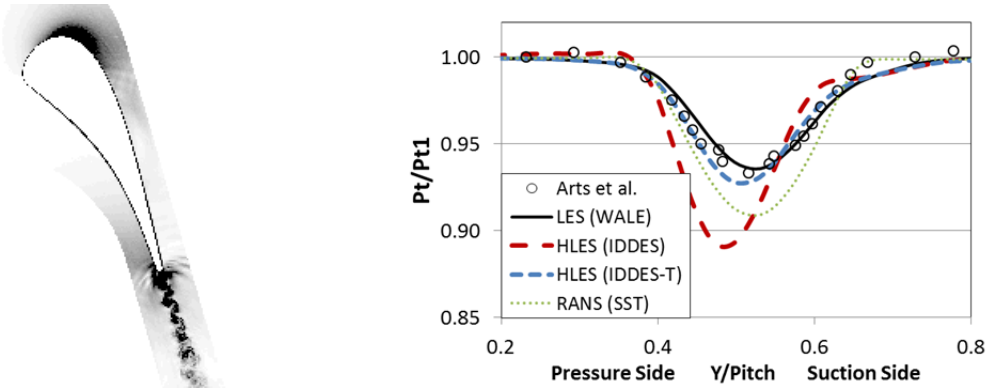

Figure 10. Wall-resolved WALE LES of a spanwise and pitchwise periodic model of the VKI uncooled S1N. (Left) "numerical Schlieren". (Right) total pressure wake at 0.43 axial chords downstream of trailing edge (Kopriva et al., 2014).

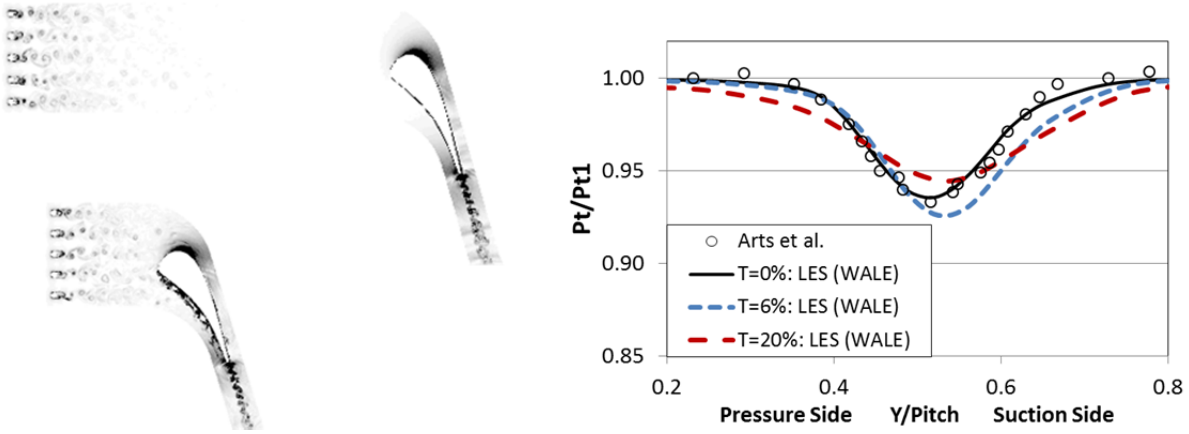

Figure 11. Wall-resolved WALE LES of a spanwise and pitchwise periodic model of the uncooled VKI S1N showing impact of turbulence grid far upstream and far downstream. (Left) numerical Schlieren. (Right) impact on total pressure wake at 0.43 axial chords downstream of trailing edge.

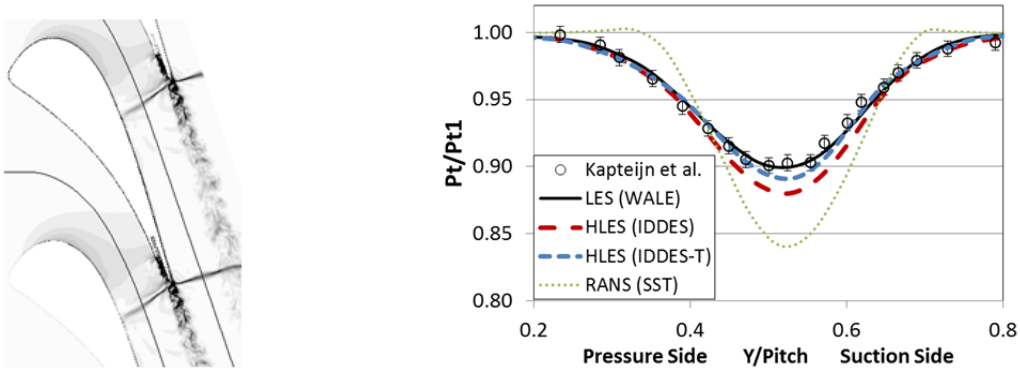

Figure 12. Wall-resolved WALE LES of a spanwise and pitchwise periodic model of the uncooled VKI S1. (Left) numerical Schlieren. (Right) impact on the total pressure wake at 0.46 axial chords downstream of trailing edge (Kopriva et al., 2014).

The trailing edge cooling for the cooled VKI vane is a simple slot. Ivanova and Laskowski (2014) executed RANS, URANS and wall-resolved LES simulations to compare back with wall heat transfer data of Kacker and Whitelaw (1968). As shown in Figure 13 RANS clearly undermixes in the shear layer off of the lip. The URANS result enables vortex shedding which facilitates faster mixing but is still significantly overpredicted. The wall-resolved LES is in excellent agreement with the data. Ivanova and Laskowski (2014) demonstrated both wall-resolved LES and DES showed excellent agreement with data for a range of geometry and flow conditions.

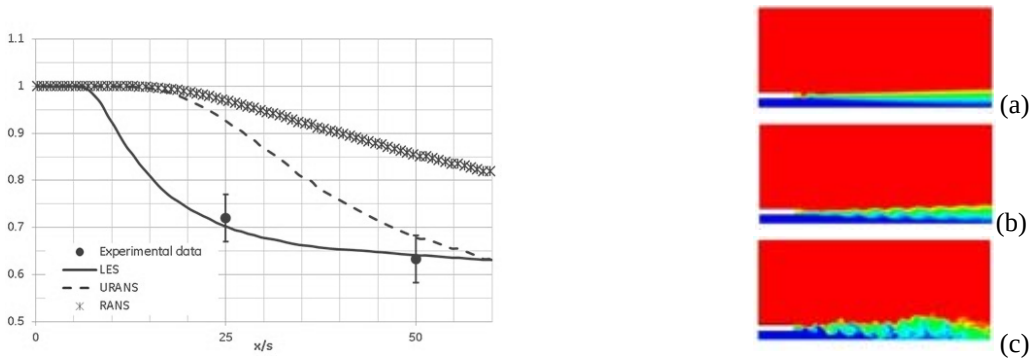

Figure 13. LES, URANS and RANS for a simplified HPT trailing edge slot cooling geometry. (a) film effectiveness on lower plate downstream breakout (b) RANS (c) instantaneous URANS (d) instantaneous WRLES.

The uncooled VKI S1N studied by Kopriva et al. (2014) motivated the study by Wheeler at al. (2015) in order to scrutinize heat transfer, detailed aerodynamics, and loss generation by first comparing with data, and then deepening the analysis based on the detailed DNS results. The simulation revealed how freestream turbulence can augment pressure side heat transfer without any clear transition to turbulence, while the suction side is characterized by a very late transition largely controlled by the intermittent development of Kelvin-Helmholtz roll-ups that eventually distort into lambda vortices prior to transition to turbulence as can be seen in the uptick of heat flux in Figure 14.

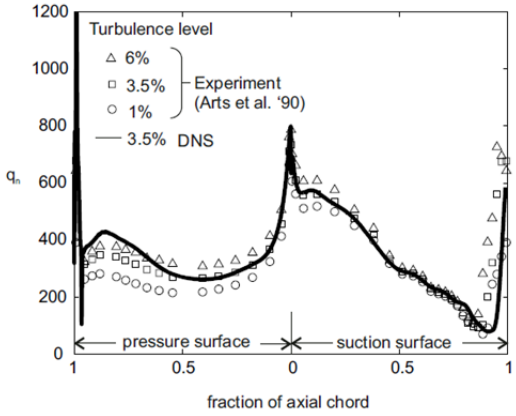

Figure 14. DNS results for heat transfer around the uncooled VKI S1N.

The pressure waves caused by the trailing edge vortex shedding generate pressure disturbances and local shocks as seen in Figure 15 that propagate upstream and trigger the onset of Kelvin-Helmholtz structures. As compared to the LPT results above, in which the deterministic unsteadiness generated by incoming wakes, interacts with turbulence to affect the overall loss generation, this result proved the importance of another type of deterministic unsteadiness, i.e. that produced by trailing edge vortex shedding. Although with a different strength with respect to the wake-profile interaction in LPT, once again the coexistence of stochastic and deterministic unsteadiness in a turbomachine was found responsible for flow features that impact performance and durability. This is a clear demonstration of utilizing high-order DNS on HPC to understand fundamental physics of important problems. The results also serve to help benchmark LES based approaches which are far more economical and can also potentially help improve physics models as will be discussed later.

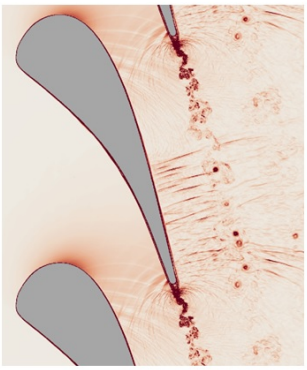

Figure 15. Contours of instantaneous numerical Schlieren for DNS of the uncooled VKI S1N.

Building off the work of Kopriva et al., (2014, 2015), a fundamental blade was designed based on the uncooled VKI vane of Arts et al. (1992). In order to simplify analysis the count was kept integral, 1:2. The objective is to conduct wall-resolved LES to further understand the implications of S1N freestream turbulence and wake on the S1B boundary layer development as shown in Figure 16. Preliminary results were shared at the 2015 APS Fluid Dynamics meeting in Boston and work is ongoing for this geometry pairing.

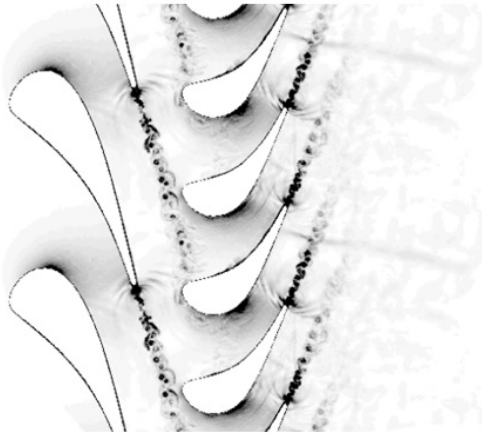

Figure 16. Unstructured Fluent hybrid LES simulation of Stage 1 HPT.

III. Numerical Algorithms

As noted earlier, aero-thermal flows in turbomachines are extremely challenging to compute because the flow is intrinsically multi-scale, unsteady, vortex-dominated, turbulent and the geometry is very complex. While RANS has been and continues to be the backbone of CFD based design, it is clear additional fidelity will be required as designs evolve. Due to the extreme cost associated with the DNS approach, variants of LES will continue to penetrate into design as computational infrastructures grow

The quality of an LES depends on the spatial filter width, the accuracy of the numerical algorithm, the computational mesh size, the time step and the accuracy of the sub-grid scale (SGS) stress model. Because of the disparate space and time scales in a turbulent flow, high-order numerical algorithms with lower dissipation and dispersion errors are attractive when compared to traditional 1^{st} or 2^{nd} order ones due to their potentially much higher accuracy and efficiency (Wang, 2007). This potential has been successfully demonstrated in the series of International Workshops on High-Order CFD Methods (Wang et al., 2013). Although high-order methods have been developed on both structured and unstructured meshes, there is a clear trend towards unstructured mesh based high-order methods because of their capability in handling complex geometries and the ability to facilitate automated mesh generation for fast design iterations and optimization, which will be discussed in the next section. Another significant advantage of unstructured meshes is the ease of domain decomposition for parallel simulations as there is no need to maintain any topology in the decomposed domains.

One of the most popular adaptive high-order methods capable of handling unstructured grids is the discontinuous Galerkin (DG) method (see e.g., Cockburn et al., 2000). Alternative approaches to high-order accuracy employing the differential form (as opposed to traditional DG which employs the integral form) have been proposed. Kopriva and coworkers pioneered this approach with the staggered-grid method on quadrilateral meshes (Kopriva and Kolias, 1996). Liu et al. (2006) developed the spectral difference (SD) method on simple meshes. Another class of schemes called spectral volume (SV) presented by Wang et al. (2004) is based on the idea of subdividing each cell into subcells or control volumes in a structured manner. A review of these as well as other types of high-order schemes can be found in (Wang, 2007).

Recently, an approach to high-order accuracy with the advantage of simplicity and economy called flux reconstruction (FR) was introduced by Huynh (2007). The FR framework unifies several existing schemes: with appropriate choices of correction terms, it recovers DG, SD, as well as SV, and the FR versions are generally simpler and more economical than the original versions. In addition, the approach results in numerous new methods that are stable and allow larger time steps than the DG method. The extension of FR to simplex and hybrid 3D meshes is carried by many researchers, e.g., in (Wang and Gao 2009, Huynh 2011, and Castonguay et al., 2012). The implementation of the FR/CPR method on GPU clusters is documented in (Zimmerman & Wang, 2014). Other recent development of the FR/CPR methods is reviewed in (Huynh et al., 2013). To present the basic idea, we consider the following 1D conservation law

$$\frac{\partial Q}{\partial t} + \frac{\partial F(Q)}{\partial x} = 0,$$

where Q is the state variable and F is the flux. In each element, the solution is defined on a set of solution points. The nodal values of the solution, $Q_{i,j}$, are used to construct a degree k polynomial denoted $Q_i(x)$. We say $Q_i(x) \in P^k$, the space of all degree k polynomials on element i. We seek to solve the governing equation in a "finite difference" manner. Therefore, we attempt to reconstruct a flux polynomial which is one degree higher than the solution, i.e., $\hat{F}_i(x) \in P^{k+1}$. Then the update follows the following a FD-like scheme

$$\frac{dQ_i(x)}{dt} = -\frac{\partial \hat{F}_i(x)}{\partial x}.$$

Given the solutions at the solution points, one can compute the flux at the solutions points, and build a flux polynomial of degree k, $\bar{F}_i(x) \in P^k$. These flux polynomials are discontinuous at element interfaces. In order to achieve conservation, the final flux polynomial must be continuous, and is computed by adding a correction polynomial of degree k+1, i.e.,

$$\hat{F}_i(x) = \bar{F}_i(x) + \sigma_i(x).$$

Depending on how the correction is formulated, the FR/CPR method can recover the DG, SV/SD methods.

In the following subsections, we address several pacing items in applying these high-order algorithms in turbomachinery analysis and design simulations.

III.1 High-Order Mesh Generation

High-order methods are not without their challenges. Meshes with straight edges or linear meshes work well for standard second-order methods. For high-order discontinuous methods, however, it was found that at solid walls, linear meshes result in a significant loss of accuracy whereas high-order meshes (i.e., with curved edges in 2D described by polynomials) work well. Another reason high-order meshes are needed is that meshes for high-order methods are considerably coarser than those for second order ones; as a result, they require curved edges in 2D and curved surfaces in 3D for accurate description of solid walls. Currently, no stand-alone commercial mesh generators are capable of generating high-order meshes. To deal with curved boundaries, a high-order meshing tool (Ims et al., 2015) has been developed to convert linear meshes into high-order ones using a surface reconstruction algorithm. The input and output format is CGNS. The key steps in the conversion are:

- Read the linear mesh in the CGNS format.
- Select patches to perform high-order reconstructions.
- Detect sharp edges, which are considered critical features.
- Reconstruct high-order polynomial representations for the selected patches. High-order reconstructions are not performed across sharp edges.
- Curve volume elements where necessary to avoid negative Jacobians.

- Save the final high-order mesh in CGNS format.

III.2 Solution Efficiency: Scalable Time Integration and Wall Modeling

Besides accuracy, solution efficiency is the other critical factor on whether these high-order methods can make an impact in design. On extreme-scale computers, we may need completely new thinking on how scalable time integration schemes look like: Will explicit schemes perform better than implicit ones? Is time accurate local time-stepping approach more efficient than global time stepping schemes?

Recent experiences indicate that for problems with a Reynolds number as high as half a million, explicit schemes with a global time stepping approach may be as competitive as implicit schemes on a few thousand compute cores. The time step size for such simulations is often determined by the smallest viscous mesh size near the wall. For explicit schemes, the CFL condition imposes a quite severe limitation on the time step size, whereas for implicit schemes, the linear solver and the associated pre-conditioner often decide the time step size. Considering that explicit schemes are much easier to parallelize, implicit schemes need to have a time step size at least one or two orders of magnitude larger to have a clear advantage over explicit ones. Research is still needed to test time accurate local time stepping approaches.

At a configuration Reynolds number on the order of tens of millions, a wall-model can potentially reduce the computational cost by several orders of magnitude. Recently, a wall-modelling approach is developed together with an implicit LES approach, and the mesh requirement was shown to be reduced by at least an order of magnitude (Zhu et al., 2016). There is potential to further improve the approach to allow y+ near the wall on the order of ~50-100. If such a model is successfully developed, we can reduce the simulation cost by several orders of magnitude for high Reynolds number flow problems.

III.3 Shock Capturing

Shock-capturing low order finite volume methods have demonstrated their capability in aircraft design. For adaptive high-order methods, there are two main approaches: limiter and artificial viscosity. There are pros and cons to each approach, and neither is fully satisfactory. The ultimate shock-capturing approach should satisfy all the following requirements:

- Accuracy preserving away from the discontinuity
- Free of user adjustable parameters
- Capable of converging to machine zero for steady problems
- Positivity preserving for pressure and density.

Although currently no approach satisfies all the requirements, there have been sufficient progresses in both approaches which allow high quality steady and unsteady simulations with shock waves to be performed. It appears that the limiter approach can be made essentially parameter free, and accuracy preserving, but is often difficult to achieve iterative convergence for steady problems, whereas the artificial viscosity approach is convergent, but not parameter free. Generally speaking, a limiter is preferred for unsteady problems, and artificial viscosity is more popular for steady problems.

Shock-capturing methods degrade to first order accuracy locally near a discontinuity because the error in the location of the shock is proportional to the mesh size. Methods which offer natural subcell resolution can make the error smaller, but cannot change the order. This argument suggests h-refinement near shock waves, coupled with a piece-wise constant reconstruction, which is the robust, first-order Godunov method. How a locally first-order scheme affects the solution elsewhere is not clear, especially for unsteady flow problems. If the mesh near a shock wave is sufficiently fine such that the magnitude of the first order error is comparable to the high-order error elsewhere with a coarser mesh, the first order method will clearly not affect the overall accuracy of the simulation. In any case, hp-adaptations for problems with shock waves appear to offer the best promise in accuracy and robustness.

For nonlinear problems without a shock wave, the shock-capturing approaches should improve the solution robustness as under-resolved smooth regions may behave as if there are shock waves there. Therefore continuous progress towards the “ultimate” shock-capturing approach is still needed.

III.4 Demonstration Examples

A Navier-Stokes solver based on the FR/CPR method (Hi-MUSIC) has been developed to conduct implicit LES at the University of Kansas, and several sample computational results are presented next using this solver.

III.4.1 Computations of bio-inspired vortex-dominated flows

This case was performed by Yu et al. (2012). A dynamic deforming mesh over a rectangular wing was used in the simulation to handle the flapping and combined flapping-pitching motion, as shown in Figure 17. In this study, the Strouhal number (*St*) of the finite-span flapping wing was selected to be well within the optimal range usually used by flying insects, birds, and fish (i.e., $0.2 < St < 0.4$). The Mach number of the free stream is set to be 0.05 to mimic incompressible flow. The Reynolds number (*Re*) based on the free stream velocity and the maximum chord length is 1200. The reduced frequency of the flapping motion is 3.5, and the Strouhal number of the wingtip is 0.38. The space discretization accuracy for the simulation is of third order, and the time integration is performed with the explicit third order TVD Runge-Kutta method.

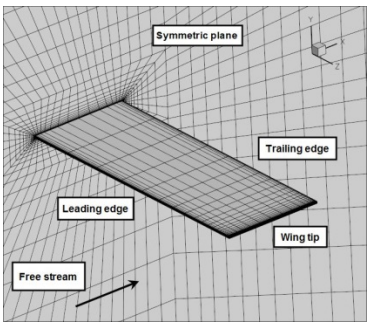

Figure 17. Wing surface and root plane meshes for a rectangular wing.

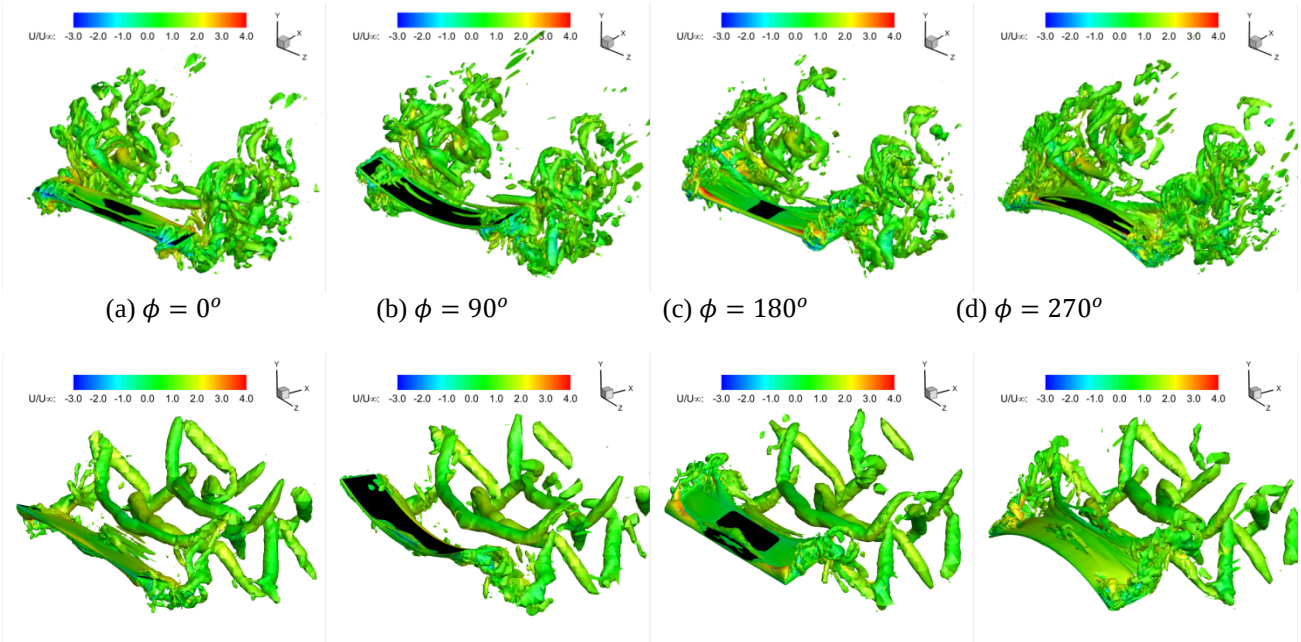

(a) $\phi = 0^o$ (b) $\phi = 90^o$ (c) $\phi = 180^o$ (d) $\phi = 270^o$

Figure 18. Comparison of the vortex topology for the rectangular and bio-inspired wings at four phases ($0^o, 90^o, 180^o$ and 270^o) with the flapping motion. Upper row: flapping motion. Lower row: flapping-pitching.

The flapping alone and the combined flapping-pitching were studied. The computed iso-surfaces of the Q-criterion at different phase angles for both motions are shown in Figure 18. Looking at the vortical structures generated by the wing motions, one may observe that more energy is wasted in the flow generated by the flapping motion due to the chaotic vortices than the one produced by the combined motion. In fact, the thrust from the combined motion is more than an order of magnitude higher than that from flapping alone. The averaged thrust from the combined motion is 27 times as large as that from the flapping motion.

III.4.2 ILES of the Transitional Flow in T106 LP Turbine Cascades

This case has been selected by the 4th International Workshop on High-Order CFD Methods as a benchmark problem, and a high-order mesh was also provided (http://how4.cenaero.be/), as shown in Figure 19a, which has 14,035 p2 hexahedral elements with 5 elements in the spanwise direction. We used FR/CPR schemes of p = 2 to p = 4 (3rd to 5th order) to assess the p-dependence of the simulations. The iso-surfaces of the Q-criterion colored by the spanwise vorticity is shown in Figure 19b for p = 3. The surface c_p distributions are displayed in Figure 20. Note that there is excellent agreement between the experimental data, HO unstructured Hi-MUSIC and HO structured FDL3Di which uses compact finite differences on overset grids (Gaitonde and Visbal, 1998). The computed wake loss profiles are compared with data in Figure 21. Again the agreement is very good.

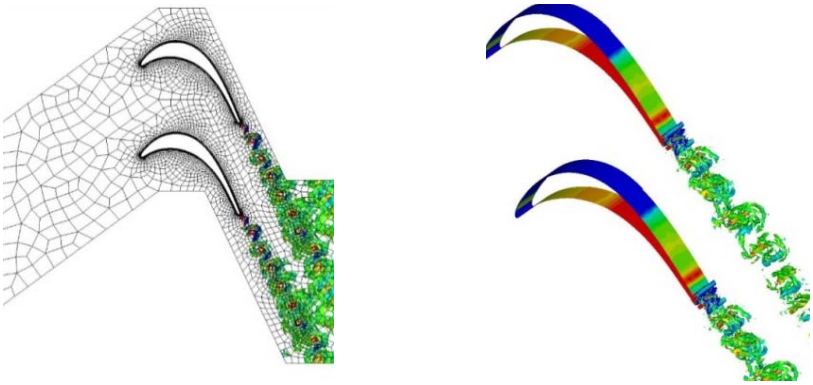

(a) (b)

Figure 19. (a) Computational mesh for T106A LPT (b) Iso-surfaces of Q-criteria colored by the spanwise vorticity

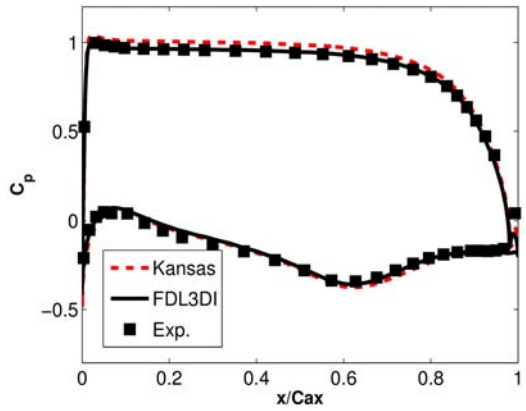

Figure 20. The surface pressure coefficient along the airfoil.

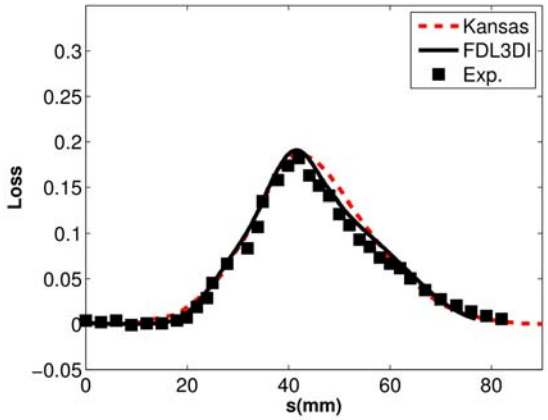

Figure 21. The comparison of computed wake loss at 40mm downstream of the trailing edge.

III.4.3 Uncooled VKI Vane Case

Again building off the work of Kopriva et al. (2014, 2015) the geometry investigated is that of Arts and Rouvroit (1992) at an isentropic exit Reynolds number approximately 584,000 and isentropic exit Mach number 0.92. The geometry and the computational mesh for this problem are displayed in Figure 22. The mesh was generated with gmsh, and contains 264,640 p2 hexahedral elements with 32 elements in the spanwise direction. FR/CPR schemes of p = 2 to p = 5 (3^{rd} to 6^{th} order) were used in the simulations to assess p-dependence of these simulations. For each element, there are $(p+1)^3$ internal degrees of freedom (DOFs). Therefore the total numbers of DOFs for p = 2 to p = 5 are 7.1M, 16.9M and 33.1M, 57.2M respectively. The numerical Schlieren distributions are compared in Figure 23, and note good qualitative agreement in instantaneous flow structures. The surface isotropic Mach number, heat transfer and turbulence intensity are compared in Figure 24.

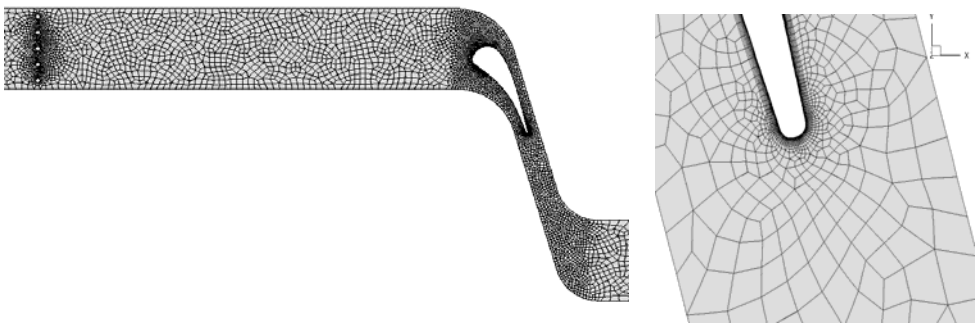

Figure 22. FR/CPR unstructured computational mesh for the uncooled VKI S1N.

(a) FDL3DI

(b) CPR-P5

Figure 23. Comparison of numerical schlieren contours ($c\left|\nabla\rho\right|/\rho$, c being the chord length).

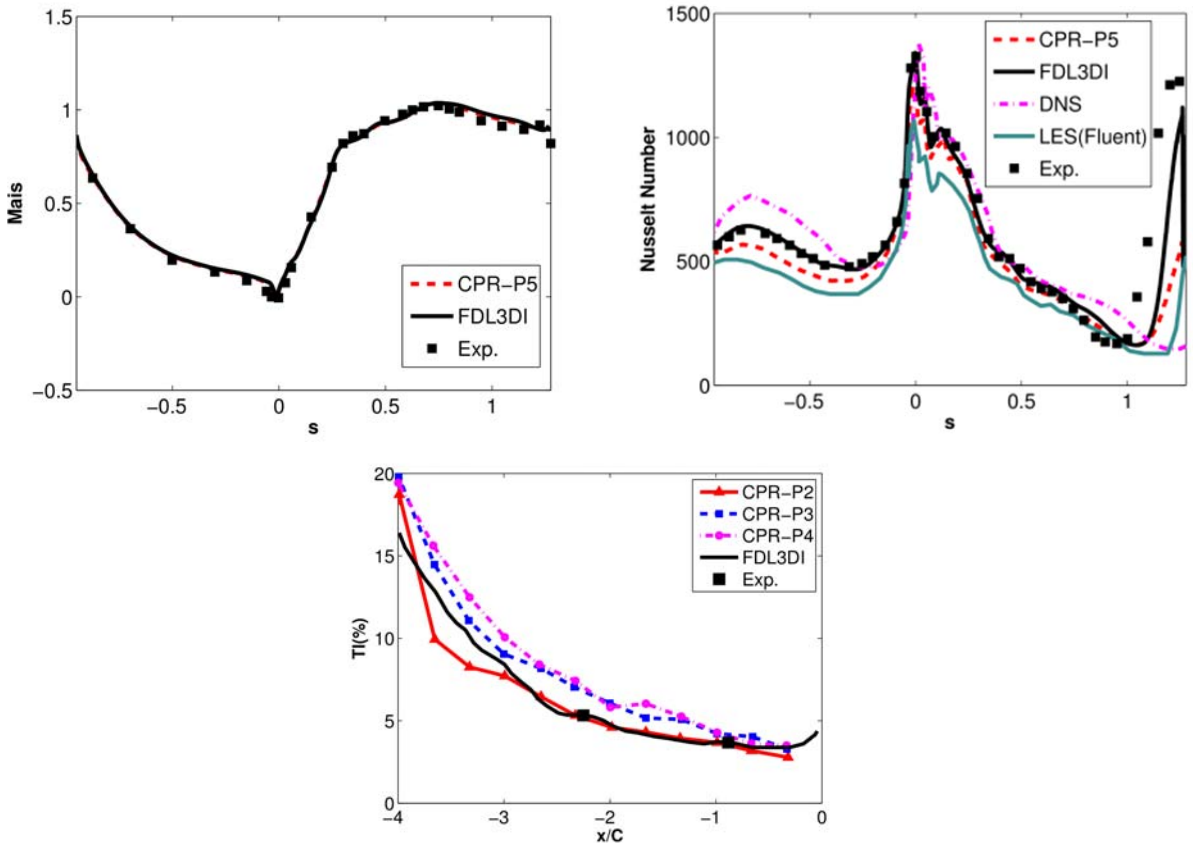

Figure 24. Comparison of surface isotropic Mach number, heat transfer and turbulence intensity upstream of the leading edge.

IV. Physics and Boundary Condition Modeling

As noted earlier, the computational cost for multi-stage turbomachinery wall-resolved LES is staggering. Over the next several years variants of LES will most likely become more commonplace not just in analysis but design when the additional accuracy is warranted. It is also quite possible that limited and targeted wall-resolved LES simulations for single blade rows will be conducted. In order to accelerate the adoption of these accurate simulation techniques significant speed up will be required. Most notably, wall models for non-equilibrium boundary layers that can capture separation in adverse pressure gradients, transition and shock-boundary layer interaction, over a wide range of Reynolds and Mach numbers will need to be developed and validated. New ideas such as those proposed by Bodart and Larsson (2011) and Bose and Moin (2014) will need to be further developed and researched extensively.

In addition to wall modeling, energy conserving phase lag boundary conditions for non-integral blade row counts will be required. Mouret et al. (2015) presented an extensive study of different techniques and demonstrated good agreement with proper orthogonal decomposing for LES simulations of flow past a circular cylinder and URANS simulations in a single-stage compressor.

While it is likely that variants of LES will become more commonplace, RANS and URANS will continue to be the workhorse for CFD based contributions to design of features, components and systems. Uncertainty quantification of boundary conditions and RANS modeling assumptions is showing promise as demonstrated by Emory et al. (2016). But as was demonstrated earlier, there are classes of problems that may require additional accuracy than what RANS and URANS can provide. This will accelerate as advances in HPC, computer science, physics models and algorithms continue to develop. It is conceivable that as variants of LES become more commonplace, large datasets will provide an opportunity to improve RANS and URANS modeling.

As an example, RANS (SST) clearly underpredicted the mixing of both the uncooled and cooled VKI S1N cases discussed previously. WALE LES modeling clearly matched the wake. Hypothesizing that the miss was due to lack of diffusion in the SST model, a meta-model assisted optimization of the diffusion coefficients on a Bayesian response surface map based on the framework described in Zlatinov and Laskowski (2015) was developed. The diffusion coefficients of the SST model were tuned for the uncooled VKI S1N to match SST mass weighted turbulent kinetic energy through the passage and the wake to time averaged resolved scale turbulence of the wall-resolved simulation. The tuned coefficients resulted in a much better wake prediction using tuned diffusion coefficients but, more importantly, when applied to the cooled VKI S1N a significantly better match was observed for that case as well as shown in Figure 25. Clearly tuning coefficients blindly has significant limitations, but this demonstrates opportunity to leverage wall-resolved LES to develop models suitable for engineering. Much more rigorous approaches using machine learning and gene programming are outlined by Tracey et al. (2015) for RANS modeling and Weatheritt and Sandberg (2015) for HLES modeling.

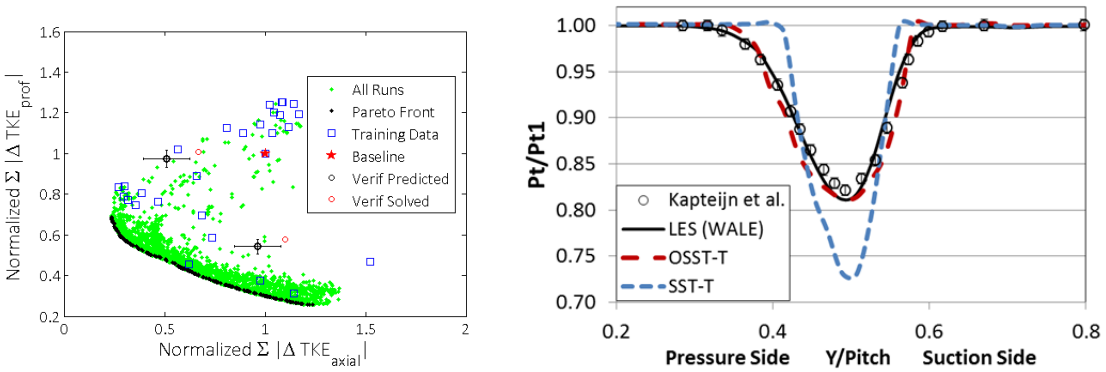

Figure 25. SST model coefficient optimization to match LES results and experimental data at 0.09 axial chords downstream of trailing edge. (Left) Pareto front for optimization on uncooled VKI S1N with objective function to match mass weighted resolved turbulent kinetic energy through S1N passage and wake. (Right) application of tuned coefficient to cooled VKI S1N.

Another opportunity for high-fidelity CFD for simplified geometries is the verification of some modeling assumptions often made in Reynolds averaging. Pichler et al. (2015) were able to postprocess their DNS and LES results analytically. Figure 26 summarizes the outcome in terms of turbulence shear stress prediction error, when using a two-equation approach for the computation of the flow in an LPT with unsteady incoming wakes generated by moving cylinders. The plot shows the difference between the resolved turbulent shear stress by DNS and the turbulent shear stress computed by using the Boussinesq assumption. The importance of this plot is that it reveals how large errors can happen away from boundary layers, i.e. in the region of the bow-apex of the incoming wakes. After being able to identify regions of modeling issues, Pichler et al. (2015) were able to dissect the different components of the turbulent shear stress tensor in the wake region. Figure 27 compares the DNS resolved turbulent shear stresses with those obtained by using a linear constitutive law and different assumptions in the computation of the turbulent viscosity. Pichler also identified ways to use DNS to produce an optimal turbulent viscosity field that minimizes the loss of accuracy with respect to DNS. While his method is not immediately able to produce a turbulence model, the results are of paramount importance as they indicate the entitlement of any given model assumption. When properly used, the approach of Pichler et al. (2015) can indicate avenues for model simple model improvements able to focus on top offenders in specific turbomachinery flow areas, like leading and trailing edges, and wakes. In the recent past Parneix (1996) attempted a similar method taking the DNS data-base of a backward facing step and scrutinizing each term of a full Reynold stress model, and attempting a recalibration of the model. The authors run into difficulties due to the non-linear response of the model to changes of the tuning constant values. A more advanced approach was used by Weatheritt and Sandberg (2015) who used symbolic regression to formulate ways to blend LES and URANS in the framework of hybrid modeling approach. Their methodology is based on the so-called “Gene-Programming”. This approach is able to define a model by scrutinizing a large number of combinations of functionals, and propose a model form that fits best a pre-defined objective.

Theory was, and still needs to be, the foundation of every turbulence model and turbulent quantities in proximity to walls must obey well known limiting forms turbulence invariants (Lumley, 1978) must be constantly considered, together with the constraints imposed by time-averaging. Nevertheless, conventional human-driven modeling is

practical in presence of experimental databases the size of which is limited in terms of both cases and depth of information. The recent and growing availability of DNS and LES of flows in realistic conditions and geometries relevant to aircraft engines allows investigating flow features that were previously only surmised based on experiments. But the large size and depth of these databases calls for a shift in turbulence modeling where machine learning can prove useful. The simple example of Weathritt and Sandberg (2015) is an example of how a hybrid LES-URANS blending function developed by Symbolic Programming based on a single DNS data base can be successfully applied to other flow fields.

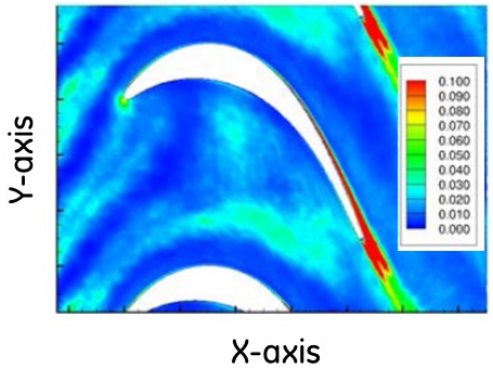

Figure 26. Reynolds stress prediction error using k-ε model and the Boussinesq approximation applied to the T106A LPT blade, Re=60K, Fred=0.61.

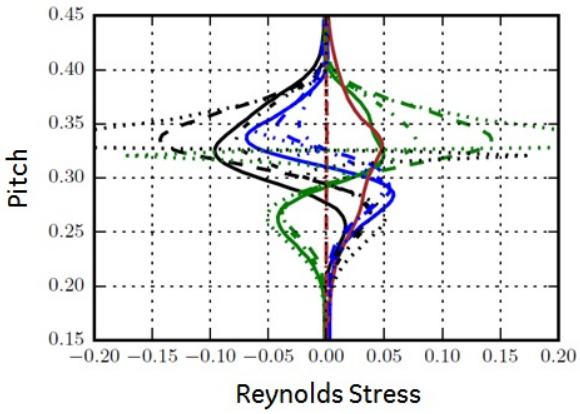

Figure 27. Comparison of Reynolds Stresses from DNS (solid lines) with modelled stresses using a linear model assumption with μ_t, k-ε computed by using DNS data (dashed lines), $\mu_{t,opt}$ computed the minimize deviations from DNS (dash-dotted lines), and μt,sh computed to minimize deviations from shear stresses only. τ11=black lines, τ12=blue lines, τ22=green lines, τ33=brown lines, downstream of T106A trailing edge.

V. Optimization & UQ

In order for simulation to be truly impactful, the ability to quickly evaluate a design space and execute trade studies is required. As discussed earlier, numerical simulations, when sufficiently validated, can enable engineers to massively increase productivity. Present day simulations on computers and engineers complement each other because they are good at fundamentally different things. Engineers are capable of quickly forming concepts and intuition, through which decisions are made and new ideas are generated. Engineers are less good at making sense of big data, enormous design parameter space and how myriad performance metrics depend on the interactions between design parameters. Modern computers are exactly the opposite: they struggle at the kind of creative thinking that lead to new solutions to engineering problems, but they excel at processing large amounts of data, algorithmically tuning many design parameters, exploring among fundamentally similar designs, and finding ones

with the best overall performance. To best complement engineers, we need to not only develop computational simulations that are reliable and vetted, but also build on top of these simulations optimization tools, algorithms that allows computers to efficiently maximize an overall performance metric within a parameterized engineering design.

In order for an optimization tool to be effective, not only must the engineer specify an accurate and complete set of objective functions and constraints, but have a reliable simulation capability at his or her disposal. As noted earlier, 0D and 1D tools, along with RANS/URANS are the backbone of modern design, but their accuracy requires expensive testing to reduce risk. High-fidelity simulations, such as variants of LES, are more trustworthy than lower fidelity ones in applications involving separated flow and turbulent heat transfer as demonstrated earlier. Optimization using these simulations, however, can be a major challenge. High-fidelity simulations can reproduce the chaotic dynamics of the underlying flow field. When a simulation runs for significantly longer time than the chaotic time scales, it can be difficult to produce smooth and accurate response surfaces for objective functions and constraints, limiting the choice of efficient optimization algorithms.

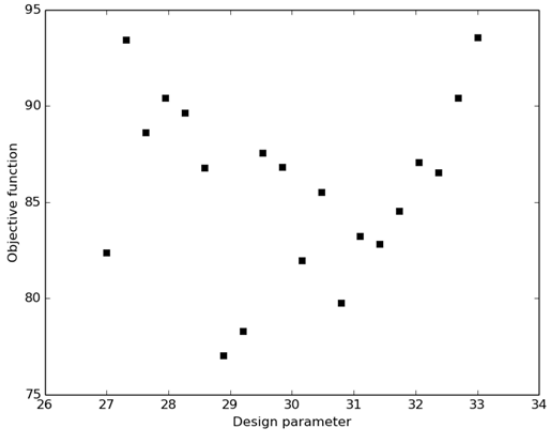

Figure 28. $\overline{(z-27)^2}$ of the Lorenz attractor, computed by averaging over 50 time units, as a function of the design parameter ρ, at $\sigma = 10$ and $\beta = \frac{8}{3}$.

Figure 28 shows how the computed objective function can have noisy dependence on design parameter in a chaotic simulation. The objective function shown in the figure is a long time average, also known as a statistic, in a simulation. Best practices call for computing such quantities by averaging over at least an order of magnitude longer than the longest time scale in the system. In this example, the objective function is averaged over 50 times the longest time scale. Even so, significant noise is apparent, making it unclear how the objective function depends on the design parameter, whether there is a local minimum, and where it is.

In a chaotic simulation, significant noise in time averaged objective function can be attributed to the sampling error, which denotes the difference between finite-time average and infinite-time average. The sampling error appears as uncorrelated noise even for very similar design parameters. This is because the sampling error depends on the history of the simulation, or the trajectory the simulation goes through in its phase space, which is extremely sensitive to design parameters in a long-time, chaotic simulation. Sampling error can be reduced by averaging longer, but at very high cost. Reducing the sampling error by a factor of 10 requires running the simulation for 100 times longer. This is because instantaneous quantities in a chaotic simulation behave like stochastic time series, and the error in its sample mean decays at the same rate of Monte Carlo methods, $O\left(T^{-\frac{1}{2}}\right)$.

Noisy sampling error in computed objective functions poses significant challenge to optimization methods. To reduce the effect of such noise, a classic approach is to fit a smooth approximation using noisy evaluations of the objective function. The resulting approximate but smooth objective function is called a surrogate model or a metamodel. Optimization is then performed on top of the well-behaved metamodel.

Zlatinov and Laskowski (2015) adopted this approach to optimize a turbulated square duct, using a hybrid large-eddy simulation turbulence modeling approach shown in Figure 29. The geometry of the turbulators is optimized for two competing aero-thermal performance metrics: heat transfer and pressure drop. The optimization starts by running an initial batch of simulations, sampled using a design of experiments in the design space. A metamodel is then fitted through these simulations, on which a Pareto front is generated. Designs on the Pareto front are then

verified with a second round of simulations. The optimization demonstrates the ability of metamodeling to handle nonlinear objective functions polluted by noisy sampling error computed from high-fidelity simulations.

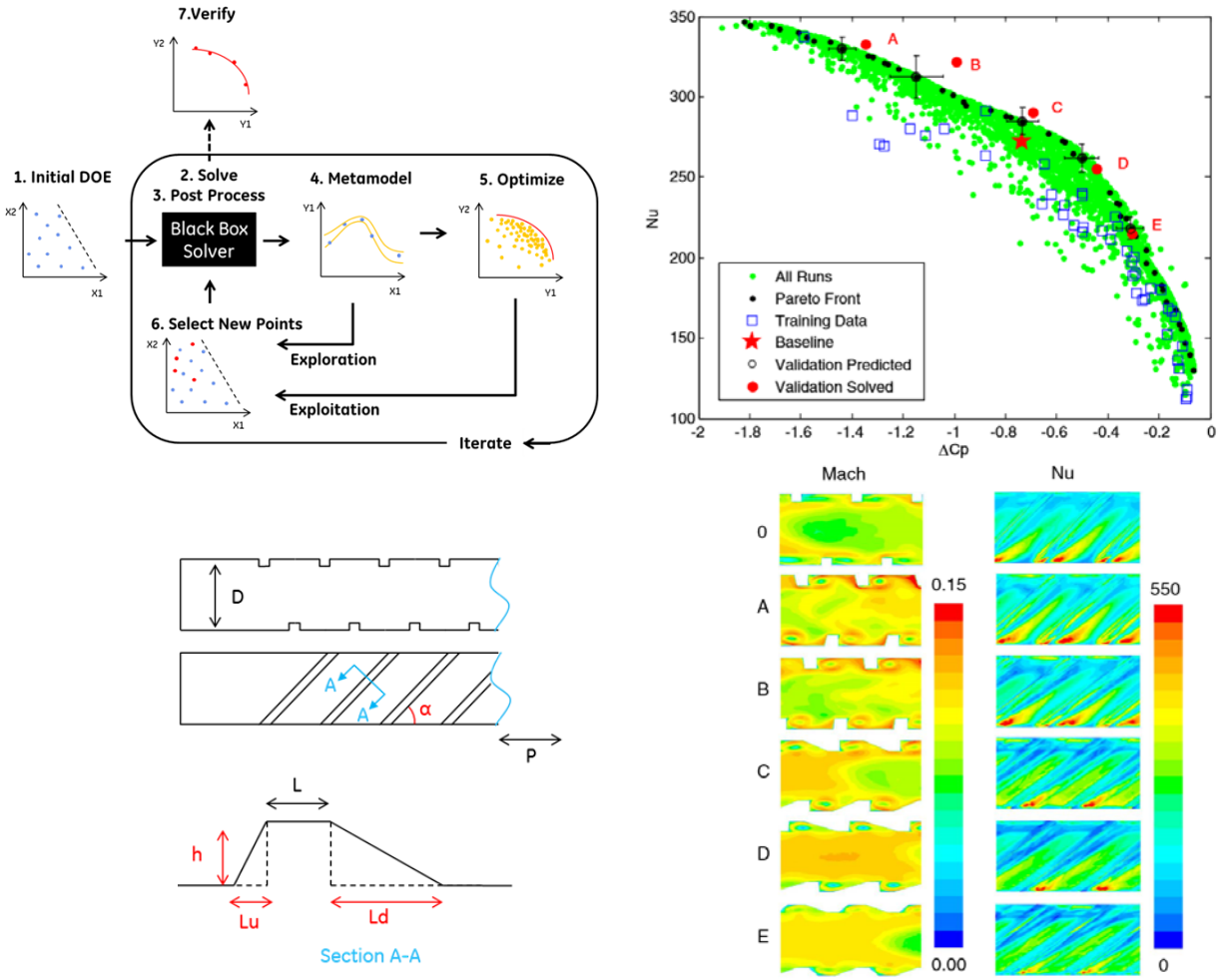

Figure 29. Optimization of a turbulated passage using HLES and Bayesian based meta-models.

A similar approach is adopted by Talnikar et al. (2016) to optimize the trailing edge geometry of the uncooled VKI S1N building off the work of Kopriva (2014, 2015). Wall-resolved Large Eddy Simulations were executed to optimize the same aero-thermal objective functions as the previous study: pressure loss and heat transfer. This optimization also starts with an initial batch of simulations, sampled using a design of experiments, on which metamodel is then fitted. A specific type of metamodel, Gaussian process regression is used, in order to provide an estimate to the amount of uncertainty in the objective function. This uncertainty estimate is then used in a Bayesian probability framework. A Bayesian algorithm is used to design additional simulations to reduce the uncertainty in the optimal design parameters. The algorithm is designed to simultaneously run several simulations, each parallelized to thousands of cores, in order to utilize additional concurrency offered by today's supercomputers. Results showed a 17% reduction on total pressure loss and 21% improvement on wall heat flux in the trailing edge region. Results of the simulations can be found in Figure 30.

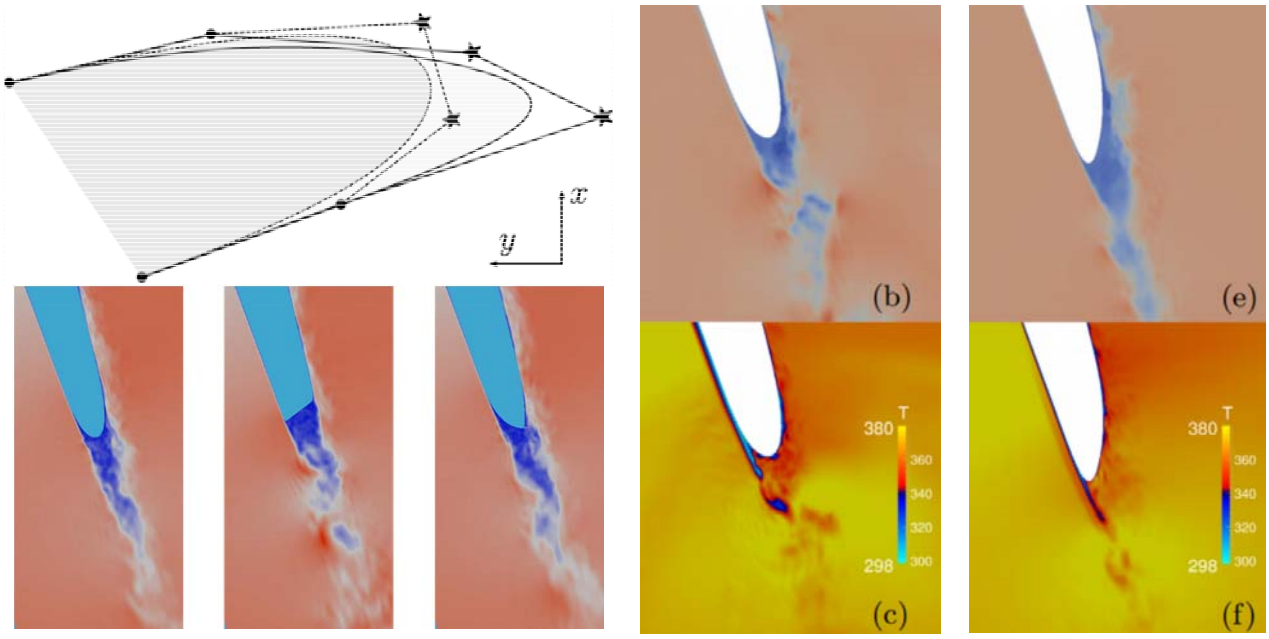

Figure 30. Optimization of the trailing edge of an uncooled HPT S1N. Upperleft: parameterization of the trailing edge via two control points (stars); lowerleft: sample geometries explored by the optimizer; Center: Mach number (upper) and temperature (lower) of the baseline design. Right: Mach number (upper) and temperature (lower) of the optimized design, with 21% less heat transfer and 17% less pressure loss compared to the baseline.

Despite showing much promise, current high-fidelity optimization methods are restricted to a small number of design parameters. Constructing global surrogate models using only samples of objective functions requires exponentially many samples in higher dimensions. Most successful optimization algorithms in higher dimensions are based on constructing local surrogate models, using local information such as gradients and Hessians of the objective function. The gradient, for example, gives the direction in the design space in which the optimization can confidently explore to further improve the objective function.

Local sensitivity analysis can be used to estimate the gradient of an objective function computed by a simulation. The adjoint method, for example, is a sensitivity analysis method that has shown promise in high-dimensional turbomachinery optimization. Marta et al. (2013) showed that the gradient can be computed at a cost almost independent of the number of variables, for a legacy (RANS) solver. They accurately computed the gradient of functions of interest, including mass flow, pressure ratio and efficiency, with respect to shape parameters, and presented the integration of such tools in an engineering design framework. Their method was applied to optimizing a compressor rotor blade passage, where the efficiency is increased by adjusting the camberline angle distribution. Sensitivity analysis combined with gradient-based optimization has been very successful for a range of non-chaotic simulations.

If efficient sensitivity analysis can be performed on chaotic, high-fidelity simulations, such as LES, it would enable high-fidelity optimization with many design variables. Consider the same example shown in Figure 31. If the derivative of the objective function can be computed it would clarify the trend of the objective function despite the noisy values – there is a clearly a local minimum where the design variable is about 30, because the derivative indicated by the slopes switches from negative to positive. Providing such gradient information efficiently in a high-dimensional design space is key to high-fidelity optimization with many design parameters.

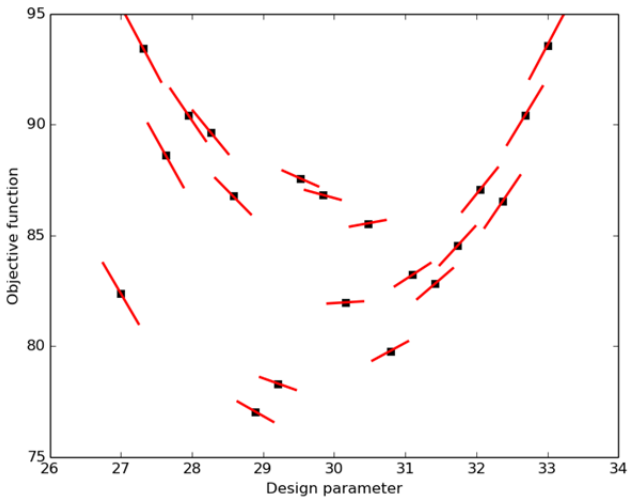

Figure 31. $\overline{(z-27)^2}$ of the Lorenz attractor, as well as its derivative computed using least squares shadowing over 50 time units, as a function of the design parameter ρ, at $\sigma = 10$ and $\beta = \frac{8}{3}$.

New methods of sensitivity analysis for chaotic simulations have recently been developed. The Least Squares Shadowing method is particularly promising. Blonigan et al. (2016) applied this method to chaotic vortex shedding of a stalled airfoil in 2D. They have shown that this method computes accurate sensitivity using only 2,000 time steps, compared to the 11,000,000 time steps required to verify the local trend of the objective function. However, the current implementation of this method costs more CPU-hours on these 2,000 time steps than 11,000,000 time steps of flow solution. Ongoing research promises to dramatically reduce the cost of the new method.

Another approach to sensitivity analysis of chaotic flow simulations, pursued by Talnikar et al (2016), is to identify local flow structures that lead to chaotic dynamics. In Large Eddy Simulation of the uncooled VKI S1N case, for example, the transition region of the boundary layer on the suction side, as well as the separated flow in the near-wake of the trailing edge, are unstable flow features that are responsible for chaotic dynamics. The chaotic dynamics cause the adjoint solution to diverge exponentially from the trailing edge region when solved backwards in time. The local regions responsible for chaotic dynamics can be identified with an energy analysis of the unsteady compressible Navier-Stokes adjoint equations. The analysis indicates that adding artificial viscosity to the adjoint equations can stabilize the adjoint energy while potentially maintain the accuracy of the adjoint sensitivities. Tests in both canonical vortex shedding and uncooled VKI S1N have indicated that high quality sensitivity can be obtained by inject just enough stabilization to prevent the divergence of the adjoint field. Ongoing research in chaotic sensitivity analysis would enable high-fidelity optimization with many design parameters.

VI. Supercomputing & Computer Science

It is conceivable that the equivalent systems to today's leadership class computing facilities like DoE Titan/MIRA and NSF Blue Waters will in the future have a combination of multi-core computing units with a tightly integrated processing unit and a low latency network back-plane. While these facilities will again be debuted in leadership class environments, as the commodity market for gaming, networked social facilities and voice/image recognition services become more common-place, the cost of these environments is expected to steadily decrease and as with linux compute environments, high-fidelity CFD will stand to benefit. To exploit this, high-fidelity CFD codes need to be able to perform on a continuum of scales in compute environments. On one end of the spectrum is the equivalent of current desktops or linux environment which will have hundreds/thousands of compute core available to a single designer or a small sub-set of the design group, transition to "clusters" which will have hundreds of thousands of cores and finally the equivalent of leadership computing which will have millions of cores. To transcend this spectrum, high-fidelity CFD codes will need research and development in the following areas.

VI.1 Multi-Core Architectures

Much work has already happened in this area as we have explored porting traditional MPI codes to OPENMP and various flavors of GPU execution. While early indications of dramatic speedup from GPUs (100X) when appropriately factored for cost/power is now shown to provide speedup of 1.3X for industrial strength codes, nevertheless, the lessons from these studies have enabled us to understand how to efficiently mix OpenMP and

processing units in conjunction with network backplanes. When the main CPU and the GPU do not share memory and when the interconnect between the two can be slow, care must be taken in how we schedule the processing units and what arrays need to be migrated between the two units. In addition, these studies have also helped us understand how to reduce/handle race conditions and how to "stride" our primary arrays to enable flux computations and matrix operations in an efficient manner. While today the two processing units are essentially two separate units and the code developer needs to use a combination of understanding of compute architectures and programming environments like OpenACC/CUDA to leverage both compute units, we believe that the future state of these machines will be a more integrated environment and support for execution embedded in standard high-level languages like Fortran/C/C++ and OPENMP standards.

VI.2 Scheduling Algorithms for Fault-Tolerant Execution

Finally, while fault-tolerant execution will be desired across the spectrum of compute environments, its need will become more important for the leadership class environment. Achieving this will require closer cooperation/collaboration between numerical analysts and computer scientists. In addition, we will need to build new programming paradigms which make it easier to encode operations like scheduling/data-exchange/recovery from faults/redundancy etc. (Kale and Bhatele, 2013). As these frame-works realize some form of standardization, we expect to see a move towards an MPI-like standard where turbomachinery designers, numerical analysts and computer scientists re-formulate the compute paradigm for high-fidelity CFD. We see this paradigm to essentially contain three layers, the scheduling/fault-tolerant layer which handles the order of execution, the numerical analyst layer which determines the choice of spatial and temporal discretization along with a library of algorithms for time-integration and a physics modeling layer that applied turbomachinery designers will choose to best approximate the fluid mechanics of interest.

VI.2 Revisit of Algorithms

As outlined in Section III, it is likely that some combination of higher-order spatial discretizations (or at least tailored second-order schemes with low dissipation and dispersion qualities) in conjunction with explicit time-stepping algorithms may form the backbone of the numerical algorithms for high-fidelity CFD codes. With the evolution of compute hardware to a more multi-core environment with shared and distributed memory, high bandwidth interconnects between compute nodes and the desire for more abstraction of the computer science aspects of the problem, simpler algorithms like explicit time-marching and "dense" FLOP methods (algorithms that have a large ratio of FLOP to communication ratio) like higher-order methods seem like a perfect match for the compute environments and software paradigms of the future.

VII. Conclusions

Computational Fluid Dynamics has made great contributions to technology development and product design for GE Aviation over the past several decades. As OPR, BR and TIT continue to increase it will put pressure on margins requiring greater understanding of fundamentals and improved accuracy of simulation tools which need to be fast in order to be effective. In order for CFD to be used in an MDAO setting, significant validation is required to gain confidence in the predictive capability. Furthermore, uncertainty due to manufacturing and transient mission operations presents a challenge for CFD and needs to be considered as part of any CFD design system.

Clearly 0D, 1D and RANS based CFD will continue to be the backbone of design systems for many years to come. As physics modeling, high-order numerical algorithms and HPC continue to advance, it is likely that variants of LES will penetrate into design for classes of problems that require the additional accuracy. High-fidelity CFD will also be used to benchmark and improve lower-order models that are massively used in design space investigations. Doing so will align general design directions indicated by improved-URANS and by LES (or DNS when possible), thereby reducing redesign.

Simplified building block examples for these methods was highlighted for various features, components and modules to focus on fundamental physics, numeric and physics modeling. Recently, GE Aviation has utilized LES and HPC to screen features and understand physics of crucial components based concepts using a numerical wind-tunnel approach. The challenge rests in system type analysis (i.e. HPT multiple stage design) where there is a need for short design iterations and understanding of engine geometry and operation uncertainties.

As noted previously, the NASA 2030 CFD vision presents a comprehensive roadmap to advance the state of the art in CFD and many aspects of that roadmap were discussed from an industry perspective. Major development efforts going forward should include:

- Supercomputing hardware growth and continued industry and academic accessibility to develop algorithms, physics models in order to demonstrate potential value for the industry
- Improvements in software to enable improved solver performance, including not just in highly parallelized compute algorithms but also in the entire software ecosystem, based on a fully holistic look at the user process from CAD import to exascale post-processing
- Capability to efficiently transform real geometry to a water tight geometry suitable for fast unstructured meshing to enable automated UQ and optimization
- Development and demonstration of robust HO unstructured algorithms for scale resolved CFD
- Development and demonstration of efficient LES wall models for non-equilibrium boundary layers, adverse pressure gradient separation, shock boundary layer interaction and transition
- Development and demonstration of energy conserving phase lag boundary conditions for variants of LES to handle non-integral airfoil counts
- Ability to optimize and execute UQ capability in both deterministic and stochastic environments
- Translate learnings of LES and DNS into improved RANS models for faster design iterations

While the focus of this paper was on aero-thermal aspects of turbomachinery, clearly combustion will be an important consideration in the development of state of the art CFD for aircraft engines which introduces complicated multi-physics challenges including radiation, combustion, chemical kinetics, soot modeling and droplet breakup and evaporation.

The opportunities for HPC and CFD to further impact the future of flight is tremendous but will require investment to mature and demonstrate new methodologies and physics models in order for them to be adopted. In addition, continued access to state of the art HPC is required to demonstrate the value of newly developed capabilities. As outlined, numerous parallels exist between areas of interest within GE Aviation and the NASA 2030 CFD vision. Strong collaboration between industry, academia and government labs will accelerate the development of the identified needs, and their adoption. Doing so will have a strongly favorable impact on the future of flight including reduced SFC, improved durability, lower emissions, and reduced noise.

Acknowledgments

The authors wish to thank the many GE collaborators who provided insight, suggestions and comments to this paper most notably Mr. Tim Stone of GE Aviation and Mr. Robert Zacharias of GE Global Research. The VKI vane LES simulations of the HPT in Section II.4 and Section III were run on NCSA Blue Waters and the authors would like to thank the Private Sector Program and the Blue Waters sustained-petascale computing project at the National Center for Supercomputing Applications (NCSA). Blue Waters is supported by the National Science Foundation (award numbers OCI 07-25070 and ACI-1238993) and the state of Illinois. An award of computer time for the LES research in Section II.1 was provided by the INCITE program. The LES research in Section II.1 used resources of the Argonne Leadership Computing Facility, which is a DOE Office of Science User Facility supported under Contract DE-AC02-06CH11357. An award of computer time for the DNS research in Section II.4 was provided by the INCITE program. The DNS research in Section II.4 used resources of the Oak Ridge Leadership Computing Facility, which is a DOE Office of Science User Facility supported under Contract DE-AC05-00OR22725.

References

Arndt, N. (1993) “Blade row interaction in a multistage low-pressure turbine”, ASME Journal of Turbomachinery, 115(1):137-146.

Arts, T., and Rouvroit, M. L. (1992) "Aero-thermal Performance of a Two-Dimensional Highly Loaded Transonic Turbine Nozzle Guide Vane: A Test Case for Inviscid and Viscous Flow Computations," ASME Journal of Turbomachinery, vol. 114.

Bodart, J. and Larsson, J. (2011) “Wall-modeled large eddy simulation in complex geometries with application to high-lift devices”, CTR Annual Research Brief.

Bodony, D. J. and S. K. Lele, (2008) “Current status of jet noise predictions using large-eddy simulation,” AIAA Journal, 2008.

Bons, J. P., Taylor, R. P., McClain, S. T. and Rivir, R. B. (2001) “The many faces of turbine surface roughness”, ASME Journal of Turbomachinery, 123(4).

Bose, S. T. and Moin, P. (2014) “A dynamic slip boundary condition for wall-modeled large-eddy simulation”, Physics of Fluids, 26.

Bunker, R. S. (2009) “The effects of manufacturing tolerances on gas turbine cooling”, ASME Journal of Turbomachinery, 131(4).

Cassagne, A., Boussuge, J-F., Villedieu, N., Puigt, G., D’Ast, I., and Genot, A. (2015) “JAGUAR: A new CFD code dedicated to massively parallel high-order LES computations on complex geometry “, FP25-2015-puigt, 50th 3AF International Conference on Applied Aerodynamics, Toulouse, France.

Castonguay, P., Vincent, P.E. and Jameson, A. (2012) “A New Class of High-Order Energy Stable Flux Reconstruction Schemes for Triangular Elements” Journal of Scientific Computing, Volume 51, Number 1, Pages 224-256.

Cockburn, B., Karniadakis, G., and Shu, C.-W., Eds., (2000) Discontinuous Galerkin methods: Theory, Computation, and Application (Springer).

Denton, J. D. (1993) “Loss mechanisms in turbomachines”, ASME Journal of Turbomachinery, 115(4):621-656.

Duggleby, A., Camp, J. and Laskowski, G. (2013) “Evaluation of massively-parallel spectral element algorithm for film cooling”, ASME GT2013-94281, San Antonio, TX.

Elmstrom, M. E., Millsaps, K. T., and Hobson, G. V. (2011) “Impact of nonuniform leading edge coatings on the aerodynamics performance of compressor airfoils”, Journal of Turbomachinery, 133(4).

Emory, M., Iaccarino, G. and Laskowski, G. M. (2016) “Uncertainty quantification in turbomachinery”, ASME GT2016-56798, Seoul, South Korea.

Ezell, S.J. and Atkinson, R.D. (2016), “The Vital Importance of HPC to US Competitiveness,” Information Technology and Innovation Foundation, http://www2.itif.org/2016-high-performance-computing.pdf

Fischberg, C. J., Rhie, C. M., Zacharias, R. M., Bradley, P. C. and DesSureault, T. M. (1995) “Using hundreds of workstations for production running of parallel CFD applications”, Parallel Computational Fluid Dynamics: Implementations and Results Using parallel Computers, A. Ecer, J. Periaux, N. Satofuka and S. Taylor (Ed.).

Gaitonde, D. V., and Visbal, M. R., (1998) “High-order schemes for Navier-Stokes equations: algorithms and implementation into FDL3DI,” Technical Report AFRL-VA-WP-TR-1998-3060, Air Force Research Laboratory, Wright-Patterson AFB, Ohio.

Gara, A. and Nair, R. (2010), “Exascale computing: What future architectures will mean for the user community,” *Parallel Computing: From Multicores and GPU's to Petascale*, IOS Press.

Garai, A., Diosady, L., Murman, S. and Madavan, N. (2015) “DNS of flow in a low-pressure turbine cascade using a Discontinuous-Galerkin spectral-element method”, ASME GT2015-42773, Montreal, Canada.

Gourdain, N., Sicot, F., Duchaine, F., and Gicquel, L. (2014) “Large Eddy simulation of flows in industrial compressors: a path from 2015 to 2035”, Philosophical Transactions of the Royal society A: Mathematical, Physical and engineering sciences, 372 (2022). ISSN 1364-503X.

Halstead, D., Wisler, D., Okiishi, T., Walker, G., Hodson, H., and Shin, H. (1997) “Boundary layer development in axial compressors and turbines: Part 1 of 4- Composite picture”, ASME Journal of Turbomachinery, 119(1):114-127.

Huynh H.T., (2007) “A flux reconstruction approach to high-order schemes including discontinuous Galerkin methods”, AIAA-2007-4079.

Huynh, H. T. (2011) “High-order methods including discontinuous Galerkin by reconstructions on triangular meshes”, AIAA-2011-44.

Huynh, H. T., Wang, Z. J., and Vincent, P. E. (2015) “High-order methods for Computational Fluid Dynamics: A brief review of compact differential formulations on unstructured grids”, AIAA 2013-2564, San Diego, CA.

Ims, J., Duan, Z., and Wang, Z.J. (2015) “meshCurve: An Automated Low-Order to High-Order Mesh Generator”, AIAA-2015-2293.

Ivanova, E. and Laskowski, G. M., (2014) “LES and hybrid RANS/LES of a fundamental trailing edge slot”, ASME GT2014-25906, Dusseldorf, Germany.

Kacker, S. C. and Whitelaw, J. H. (1968) “The effect of slot height and slot-turbulence intensity on the effectiveness of the uniform density, two-dimensional wall jet”, Journal of Heat Transfer, no 11:469-475.

Kale, L. V. and Bhatele, A. (2013) “Parallel science and engineering applications: The Charm++ approach”, Taylor and Francis Group, CRC Press, Nov. 2013.

Kapteijn, C., Amecke, J. and Michelassi, V., (1996) "Aerodynamic Performance of a Transonic Turbine Guide Vane with Trailing Edge Coolant Ejection: Part I - Experimental Approach," ASME Journal of Turbomachinery, vol. 118, pp. 519-528.

Khalighi, Y., Nichols, J. W., Ham, F., Lele, S. K. and Moin, P. (2010) “Unstructured large eddy simulation for prediction of noise issued from turbulent jets in various configurations”, AIAA 2011-2886, Portland, Oregon.

Kopriva, D. A. and Kolias, J. H. (1996) “A conservative staggered-grid Chebyshev multidomain method for compressible flows”, J. Comput. Phys. 125, 244.

Kopriva, J., Laskowski, G. M., and Sheikhi, M. R. H., (2014) "Computational Assessment of Inlet Turbulence on Boundary Layer Development and Momentum/ThermalWakes for High Pressure Turbine Nozzle and Blade," IMECE2014-38620, Montreal, Canada.

Kopriva, J., Laskowski, G. M., and Sheikhi, M. R. H., (2015) “Hybrid LES of a High Pressure Turbine". ERCOFTAC Workshop. Limassol, Cyprus.

Lattime, S. B. and Steinetz, B. M. (2002) “Turbine engine clearance control systems: current practices and future directions”, NASA TM-2002-211794, September, 2002.

Launder, B., E. and Spalding, D. B. (1974) “The numerical computation of turbulent flows”, Comp. Math. App. Mech. Engg., vol 3:269-289.

Leggett, J., Priebe, S., Sandberg, R., Michelassi, V. and Shabbir, A. (2016) “Detailed investigation of RANS and LES predictions of loss generation in an axial compressor cascade at off design incidences”, ASME GT2016-57972, Seoul, South Korea.

Liu, Y., Vinokur, M. and Wang, Z. J. (2006) “Discontinuous Spectral Difference Method for Conservation Laws on Unstructured Grids”, J. Comput. Phys., 216, 780–801.

Lopez-Morales, M. R., Bull, J., Crabill, J., Economon, T. D., Manosalvas, D., Romero, J., Sheshadri, A., Watkins II, J. E., Williams, D., M., Palacios, F. and Jameson, A. (2014) “Verification and validation of HiFiLES: a High Order LES unstructured solver on multi-GPU platforms”, AIAA-2014-31698.

Lu, Y. and Dawes, W. N. (2015) “High order Large Eddy Simulations for a transonic turbine blade using hybrid unstructured meshes”, ASME GT2015-42283, Montreal, Canada.

Lumley, J. L., (1978) “Computational modeling of turbulent flows”, Advances in Applied Mechanics, vol 18:123-176.

Mangani, L., Launchbury, D. R., Casartelli, E. and Romanelli, G. (2015) “Development of high order LES solver for heat transfer applications based on the open source OPENFOAM framework”, ASME GT2015-43279, Montreal, Canada.

Marta, A. C. and Shankaran, S. (2013) “On the handling of turbulence equations in RANS adjoint solvers”, Computers and Fluids, 74:102-113.

Marty, J., Lantos, N., Michel, B. and Bonneau, V. (2015) “LES and hybrid RANS/LES simulation of turbomachinery flows using high order methods”, ASME GT2015-42134, Montreal, Canada.

Medic, G., and Sharma, O. P., (2012), “Large-Eddy Simulation of Flow in a Low-Pressure Turbine Cascade,” ASME GT2012-68878.

Michelassi, V., Martelli, F., Dénos, R., Arts, T., and Sieverding, C. H. (1999), "Unsteady Heat Transfer in Stator–Rotor Interaction by Two-Equation Turbulence Model", ASME Journal of Turbomachinery, vol. 121, no. 3.

Michelassi, V., Wissink, J.G., and Rodi, W. (2003) “Direct Numerical Simulation, Large Eddy Simulation and Unsteady Reynolds Averaged Navier-Stokes Simulations of Periodic Unsteady Flow in a Low-Pressure Turbine Cascade: A Comparison”, (2003), Proc Instn Mech Engrs, Vol. 217, Part A: J. Power and Energy.

Michelassi, V., Chen, L., Pichler, R. and Sandberg, R.D. (2015) “Compressible Direct Numerical Simulation of Low-Pressure Turbines: Part II – Effect of Inflow Disturbances”, ASME Journal of Turbomachinery, July 2015, Vol. 137.

Moin, P. (2014) “Progress and challenges in numerical simulation of multi-physics turbulent flows in aerospace applications”, Presentation at Royal Academy of Engineering, Spain.

Montomoli, F. (2015) “Uncertainty quantification in Computational Fluid Dynamics and aircraft engines”, SpringerBriefs in Applied Sciences and Technologies.

Mouret, G., Gourdain, N. and Castillon, L. (2015) “Adaptation of phase-lagged boundary conditions to Large Eddy Simulation in turbomachinery configurations”, ASME Journal of Turbomachinery, 138(4).

Mustain, C. et al. (2014), “Solve: The Benefits of Supercomputing Investment for US Industry,” Council on Competitiveness.

Paliath, U., Shen, H., Avancha, R. and Shieh, C., (2011) “Large Eddy Simulation for jets from chevron and dual flow nozzle,” 17th AIAA Aeroacoustics conference, AIAA-2011 -2881.

Paliath, U. and Premasuthan, S. (2013) “Large Eddy Simulation for Jet Installation Effects,” 19th AIAA Aeroacoustics conference, AIAA-2013-2137.

Parneix, S., Laurence, D. and Durbin, P. (1996) “Second moment closure of the backstep flow database”, CTR summer school briefs, 1996.

Pichler, R., Sandberg, R. D., Michelassi, V. and Bhaskaran, R. (2015) “Investigation of the accuracy of RANS to predict the flow through a low-pressure turbine”, ASME GT2015-43446.

Pichler, R., Kopriva, J., Laskowski, G., Michelassi, V. and Sandberg, R. (2016) “Highly resolved LES of a linear HPT vane cascade using structured and unstructured codes”, ASME GT2016-57189.

Rodebaugh, G., Stratton, Z., Benson, M., and Laskowski, G. M. (2015) “Assessment of Large Eddy Simulation predictive capability for compound angle round film holes”, ASME GT2015-43602, Montreal, Canada.

Sandberg, R.D., Pichler, R., Chen, L., Johnstone, R. and Michelassi, V. (2015) “Compressible Direct Numerical Simulation of Low-Pressure Turbines: Part I – Methodology”, ASME Journal of Turbomachinery, May 2015, Vol. 137.

Schnell, R., Lengyel-Kampmann, T., and Nicke, E. (2014) “On the impact of geometry variability on fan aerodynamic performance, unsteady blade row interaction, and its mechanical characteristics”, ASME Journal of Turbomachinery, 136(9).

Schwaenen, M., Meador, C. M., Camp, J. L., Jagannathan, S. and Duggleby, A. (2010) “ Massively-Parallel Direct Numerical Simulation of Turbine Vane Endwall Horseshoe Vortex Dynamics and Heat Transfer”, ASME GT2011-45915, Vancouver, Canada.

Slotnick, J., Khodadoust, A., Alonso, J., Darmofal, D., Gropp, W., Lurie, E. and Mavriplis, D. (2014) “CFD vision 2030 study: A path to revolutionary computational aerosciences”, NASA/CR-2014-218178.

Stadtmueller, P. and Fottner, L. (2001) “A Test Case for the Numerical Investigation of Wake Passing Effects on a Highly-Loaded LP Turbine Cascade Blade,” ASME 2001-GT-0311.

Talnikar, C., Wang, Q. and Laskowski, G. M. (2016) “Unsteady adjoint of pressure loss for a fundamental transonic turbine vane”, ASME GT2016-56689, Seoul, South Korea.

Tracey, B., Duraisamy, K. and Alonso, J. (2015) “A machine learning strategy to assist turbulence model development”, AIAA 2015-1287.

US Dept. of Energy, Advanced Scientific Computing Advisory Committee Subcommittee on exascale Computing, The Opportunities and Challenges of Exascale computing, Fall (2010), http://science.energy.gov/ascr/ascac/

Wang, Z. J., Zhang, L. and Liu, Y. (2004) “Spectral (finite) volume method for conservation laws on unstructured grids IV: extension to two-dimensional Euler equations”, J. Comput. Phys., 194, No. 2, pp. 716–741.

Wang, Z. J. and Gao, H. (2009) “A Unifying Lifting Collocation Penalty formulation including the discontinuous Galerkin, spectral volume/difference methods for conservation laws on mixed grids”, J. Comput. Phys., 228, No. 2, pp. 8161–8186.

Wang, Z. J. (2007) “High-order methods on unstructured grids for Navier-Stokes equations,” Journal of Progress in Aerospace Sciences, Vol. 43, pp. 1–41.

Wang, Z. J., Fidkowski, K. J., Abgrall, R., Bassi, F., Caraeni, D., Cary, A., Deconinck, H., Hartmann, R., Hillewaert, K., Huynh, H.T., Kroll, N., May, G., Persson, P. O., van Leer, B., and Visbal, M. (2013) “High-Order CFD Methods: Current Status and Perspective,” International Journal for Numerical Methods in Fluids, 72, 811-845.

Warwick, G. (2014) “Digital twin would track aircraft health through its life”, Aviation Week, August 14, 2014.

Weatheritt, J. and Sandberg, R., (2015) “Use of Symbolic Regression for Construction of Reynolds-Stress Damping Functions for Hybrid, RANS/LES”, AIAA SciTech 2915, Kissimmee, FL, USA.

Wheeler, A. P. S., Sandberg, R.D., Sandham, N.D., Pichler, R., Michelassi, V. and Laskowski, G. (2015) “Direct Numerical Simulation of a High-Pressure Turbine Vane”, ASME Journal of Turbomachinery, July 2016, Vol. 138.

Wiart, C. C., Hillewaert, K., Lorriaux, E. and Verheylewegen, G. (2015) “Development of a discontinuous Galerkin solver for high quality wall-resolved/modelled DNS and LES of practical turbomachinery flows on fully unstructured meshes”, ASME GT2015-43428, Montreal, Canada.

Yu, M., Wang, Z. J., and Hu, H. (2012) “High-Fidelity Flapping-Wing Aerodynamics Simulations with a Dynamic Unstructured Grid Based Spectral Difference Method,” Proceedings of the 7th International Conference on Computational Fluid Dynamics, ICCFD7-4104.

Zhu, H., Fu, S., Shi, L., and Wang, Z.J., “Hybrid RANS-Implicit LES Approach for the High-Order FR/CPR Method”, accepted by AIAA Journal.

Zimmerman, B.J. and Wang, Z.J. (2014) “The efficient implementation of correction procedure via reconstruction with graphics processing unit computing”, Computers & Fluids, 101 263–272.

Zlatinov, M. and Laskowski, G. M., (2015) “Hybrid Large Eddy Simulation optimization of a fundamental turbine blade cooling passage”, AIAA Journal of Propulsion and Power, 31(5):1292-1297.